Science of the Total Environment 945 (2024) 173846

Contents lists available at ScienceDirect

Science of the Total Environment

journal homepage: www.elsevier.com/locate/scitotenv

The effects of climate and soil depth on living and dead bacterial communities along a longitudinal gradient in Chile

Xiuling Wang [a], Lars Ganzert [a,1], Alexander Bartholomäus [a], Rahma Amen [a,b], Sizhong Yang [a], Carolina Merino Guzmán [c], Francisco Matus [d,e], Maria Fernanda Albornoz [f], Felipe Aburto [g], Rómulo Oses-Pedraza [h], Thomas Friedl [i], Dirk Wagner [a,j,*]

[a] GFZ German Research Centre for Geosciences, Section Geomicrobiology, 14473 Potsdam, Germany
[b] Department of Zoology, Faculty of Science, Aswan University, 81528 Aswan, Egypt
[c] Center of Plant, Soil Interaction and Natural Resources Biotechnology, BIOREN, Universidad de La Frontera, Temuco 4780000, Chile
[d] Laboratory of Conservation and Dynamics of Volcanic Soils, Department of Chemical Sciences and Natural Resources, Universidad de La Frontera, Temuco 4780000, Chile
[e] Network for Extreme Environmental Research (NEXER), Universidad de La Frontera, Temuco 4780000, Chile
[f] Laboratorio de Investigación de Suelos, Aguas y Bosques (LISAB), Universidad de Concepción, Concepción, Chile
[g] Pedology and Soil Biogeochemistry Lab, Soil and Crop Sciences Department, Texas A&M University, College Station, TX, USA
[h] Centro Regional de Investigación y Desarrollo Sustentable de Atacama, Universidad de Atacama (CRIDESAT UDA), Copayapu 484, Copiapó 1530000, Chile
[i] Department of Experimental Phycology and Culture Collection of Algae (EPSAG), Albrecht-von-Haller-Institute for Plant Sciences, Georg August University, 37073 Göttingen, Germany
[j] Institute of Geosciences, University of Potsdam, 14476 Potsdam, Germany

HIGHLIGHTS

- Only a small fraction of the microbial community represented by tDNA consisted of living microorganisms.
- iDNA and eDNA communities adapted differently to climate and depth, with depth significantly affecting the iDNA community.
- The formation of microbial modules was deterministic and strongly linked to climate.

GRAPHICAL ABSTRACT

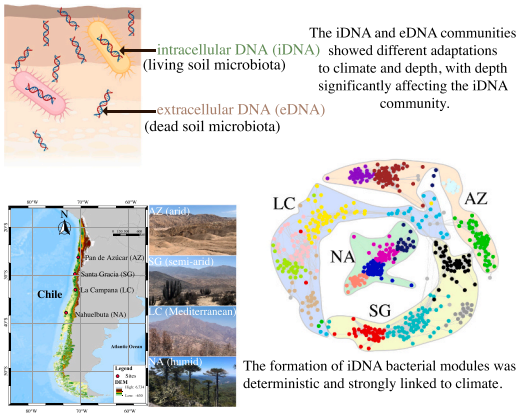

ARTICLE INFO

Editor: Elena Paoletti

ABSTRACT

Soil bacterial communities play a critical role in shaping soil stability and formation, exhibiting a dynamic interaction with local climate and soil depth. We employed an innovative DNA separation method to characterize

* Corresponding author at: GFZ German Research Centre for Geosciences, Section Geomicrobiology, 14473 Potsdam, Germany.
E-mail address: dirk.wagner@gfz-potsdam.de (D. Wagner).
[1] Current address: Leibniz-Institute of Freshwater Ecology and Inland Fisheries, Department of Plankton and Microbial Ecology, 16775 Neuglobsow, Germany.

https://doi.org/10.1016/j.scitotenv.2024.173846
Received 5 March 2024; Received in revised form 3 June 2024; Accepted 6 June 2024
Available online 12 June 2024

Keywords:
Deep soil bacterial community
Microbial diversity
Climate gradient
16S rRNA sequencing
Extracellular DNA (eDNA)
Intracellular DNA (iDNA)

microbial assemblages in low-biomass environments such as deserts and distinguish between intracellular DNA (iDNA) and extracellular DNA (eDNA) in soils. This approach, combined with analyses of physicochemical properties and co-occurrence networks, investigated soil bacterial communities across four sites representing diverse climatic gradients (i.e., arid, semi-arid, Mediterranean, and humid) along the Chilean Coastal Cordillera. The separation method yielded a distinctive unimodal pattern in the iDNA pool alpha diversity, increasing from arid to semi-arid climates and decreasing in humid environments, highlighting the rapid feedback of the iDNA community to increasing soil moisture. In the arid region, harsh surface conditions restrict bacterial growth, leading to peak iDNA abundance and diversity occurring in slightly deeper layers than the other sites. Our findings confirmed the association between specialist bacteria and ecosystem-functional traits. We observed transitions from *Halomonas* and *Delftia*, resistant to extreme arid environments, to Class AD3 and the genus *Bradyrhizobium*, associated with plants and organic matter in humid environments. The distance-based redundancy analysis (dbRDA) analysis revealed that soil pH and moisture were the key parameters that influenced bacterial community variation. The eDNA community correlated slightly better with the environment than the iDNA community. Soil depth was found to influence the iDNA community significantly but not the eDNA community, which might be related to depth-related metabolic activity. Our investigation into iDNA communities uncovered deterministic community assembly and distinct co-occurrence modules correlated with unique bacterial taxa, thereby showing connections with sites and key environmental factors. The study additionally revealed the effects of climatic gradients and soil depth on living and dead bacterial communities, emphasizing the need to distinguish between iDNA and eDNA pools.

1. Introduction

Prokaryotic soil microorganisms play a pivotal role in the material cycle of soils by contributing to mineral weathering, soil agglomeration, organic matter decomposition, and nutrient cycling (Six et al., 2004; Smith et al., 2015). These microorganisms constitute a significant portion of soil organic matter and account for approximately half its total content. Soil bacteria are a crucial component of biodiversity and represent about 25 % of all global species. The diversity of soil microorganisms is closely linked to the overall functioning of ecosystems (Guerra et al., 2021). Therefore, understanding the mechanisms that cause variations in soil microbial diversity across various geographic, temporal, and environmental gradients is a crucial research objective (Zhou et al., 2016).

Climate controls soil microbial communities through various factors, such as temperature, sunlight, and precipitation (An et al., 2023; Ruan et al., 2023; Yu et al., 2023). For instance, adding water to dry soil can stimulate the growth of microbial communities (Chase et al., 2018; Dusek et al., 2018; Tibbett et al., 2019; Rodríguez et al., 2024). The climate also indirectly affects soil microbial distribution by influencing physicochemical properties, including soil texture, erosion rate, total organic carbon (TOC) content, and pH (Rofner et al., 2017; Chase et al., 2018; Naylor et al., 2020). Soil microbes can additionally rapidly adapt to resource shifts caused by climate change (Van Horn et al., 2014; Lee et al., 2018).

Soil depth also plays a significant role in shaping soil microbial communities, with distinct physicochemical property gradients (e.g., soil texture, organic matter, moisture, and oxygen) capable of being observed across soil layers (Lavahun et al., 1996; Meier et al., 2019; Mundra et al., 2021). The biomass of microbial communities in deeper soil layers is often less abundant than that in surface soil layers due to the limited availability of carbon sources (Erich et al., 2012). Additionally, soil oxygen content decreases with depth (Paul, 2014), directly impacting microbial metabolism (Schellenberger et al., 2010). These climate and depth gradients provide a valuable perspective when investigating the organization of soil microbial biomes in different environments (Naylor et al., 2020; Xu et al., 2021).

With its extensive latitudinal range and diverse climatic zones, Chile offers an ideal location for cross-climate research (Beck et al., 2018). The Chilean Coastal Mountain Range provides a consistent siliciclastic soil parent material that spans various climate gradients (*Geological Map of South America at a Scale of 1:5M*, 2019). For example, soil properties such as clay content, organic carbon, total DNA, and pH exhibit distinct variations throughout the climatic zones along Chile's west coast (Bernhard et al., 2018). Microbial diversity in shallow subsurface soils along the Chilean Coastal Cordillera is primarily influenced by pH and carbon/nitrogen (C/N) ratios (Rodriguez et al., 2022). However, most current research focuses on microorganisms in surface soil layers and their response to local climatic conditions (Ladau et al., 2018; Hao et al., 2021). Therefore, a knowledge gap exists regarding our understanding of microbial communities in deeper soil layers across different climatic zones. While climate and soil depth play significant roles in shaping soil microbial communities, it remains unclear which factor exerts a more substantial influence (Rodriguez et al., 2022).

Soil contains intracellular DNA, which is present in living, potentially active cells, and extracellular DNA, which is mostly from dead and depleted cells (Carini et al., 2016; Bairoliya et al., 2022). Extracellular DNA (eDNA) is released from cells through active or passive mechanisms (e.g., cell lysis) and can persist in the soil for weeks to millennia (Levy-Booth et al., 2007; Torti, Lever, and Jørgensen 2015; Fang et al., 2021; Pathan et al., 2021b). However, sequencing total DNA (tDNA) without distinguishing between iDNA and eDNA can lead to misinterpretations, particularly in low-biomass environments. While the number of studies on iDNA and eDNA has increased in recent years (Genderjahn et al., 2021; Pathan et al., 2021a; Schulze-Makuch et al., 2021; Medina Caro et al., 2023; Horstmann et al., 2024), the application of the separation method in climatic and depth gradients remains an understudied.

This study employs an innovative DNA separation technique to overcome the limitations of traditional total DNA methods in assessing microbial diversity and community structures in the soil. By distinguishing between living and dead bacteria, we hypothesized that a more precise revelation of how climate change and soil depth influence microbial community composition and diversity could be achieved. We further hypothesize that the iDNA communities of soil bacteria will show significant differences from eDNA communities and that specific environmental variables, such as precipitation, soil moisture content, ecological or climatic types, and soil depth, may influence these two community pools to varying degrees. Combined with physicochemical property analysis and network analytical techniques, this technique is expected to unveil the complex interactions between microbes and environmental factors, offering more profound insights into ecosystem functions.

2. Materials and methods

2.1. Study sites and sampling process

Within the framework of the German–Chilean EarthShape project (www.earthshape.net), we selected four study sites along the Chilean coast that represented distinct climatic conditions: the arid Pan de

Azúcar (AZ), the semi-arid Santa Gracia (SG), the Mediterranean La Campana (LC), and the humid Nahuelbuta (NA) (Fig. 1, Table S1). The vegetation at these sites ranged from almost none (AZ) and desert scrubs (SG) to sclerophyllous forest (LC) and temperate forest (NA) (Oeser et al., 2018).

Three replicate soil pits were excavated at each study site with a separation of 50–400 m between each pit to reduce within-site potential spatial variability. Soil samples were collected from a depth of 0–200 cm (various depths within each soil pit that encompassed the depth layers of 0–5 cm, 5–10 cm, 10–20 cm, 20–40 cm, 40–60 cm, 60–80 cm, 80–100 cm, 100–120 cm, 120–140 cm, 140–180 cm, and 180–200 cm). All samples were immediately sealed in sterile plastic bags and stored at 4 °C in Styrofoam boxes. Upon arrival in Germany, the samples were constantly maintained at 4 °C for further analysis.

2.2. DNA extraction and quantitative PCR

DNA extraction was performed using an improved method based on the protocol developed by Alawi et al. (Alawi et al., 2014). Sterivex 0.22-μm filter units (EMD Millipore Corporation, USA) separated the intracellular DNA (iDNA) and extracellular DNA (eDNA). The iDNA extraction was adapted from Nercessian et al. (Nercessian et al., 2005), while 6 M Guanidine hydrochloride (GuaHCl) and silica slurries were used to isolate and extract the eDNA. The detailed DNA extraction procedure is based on the methodology outlined by Medina Caro et al. (Medina Caro et al., 2023).

Quantitative PCR (qPCR) was performed using the CFX Connect Real-Time System (Bio-Rad Laboratories Inc., Hercules, CA, USA) to quantify bacteria in the iDNA and eDNA samples. Three technical replicates were conducted per sample targeting a universally conserved 16S rRNA gene. Each 20-μl qPCR reaction included 10 μl KAPA SYBR® FAST Master Mix (2×), 5 μl DNA template, 4.2 μl PCR H_2O, and 0.4 μl of each primer Eub341-For (CCTACGGGAGGCAGCAG) and Eub534-Rev (ATTACCGCGGCTGCTGG), both at 10 μM. The qPCR protocol included initial denaturation at 95 °C for 3 min, followed by 35 cycles of denaturation (95 °C, 3 s), annealing (60 °C, 20 s), extension (72 °C, 30 s) and an additional 3 s incubation at 80 °C. Amplification efficiency exceeded 95 %, with the standard curve correlation coefficient of ≥0.997. The standard was a known concentration of a 16S rRNA gene PCR fragment of *Bacillus subtilis*.

2.3. Library preparation and sequencing

PCR amplified the highly variable V4 region of the 16S rRNA gene using universal primers Uni515-For (GTGTGYCAGCMGCCGCGGTAA) and Uni806-Rev (CCGGACTACNVGGGTWTCTAAT). Each 50 μl of PCR reaction included 5 μl of 10× Pol Buffer C (EURx, Gdańsk, Poland), 2 μl of dNTP Mix (5 mM each), 2 μl of $MgCl_2$ (25 mM), 0.5 μl of Optitaq Polymerase (5 U/μl) (EURx), 1.25 μl of primer (10 μM) with oligonucleotide barcode (Microsynth AG, Balgach, Switzerland), 0.25 μl of BSA (20 mg/μl) (New England Biolabs, MA, USA), 30.25 μl of PCR H_2O, and 5 μl of DNA template. PCR amplification was performed in a T100TM Thermal Cycler (Bio-Rad Laboratories Inc., USA) with the following cycling program: initial denaturation at 95 °C for 5 min, followed by 30 cycles of denaturation at 95 °C for 30 s, annealing at 55 °C for 30 s, elongation at 72 °C for 45 s, and final elongation at 72 °C for 10 mins. PCR products were purified using a magnetic bead-based kit (High-Prep™ PCR Clean-up System, MAGBIO Genomics Inc., MD, USA) following the manufacturer's recommendations. PCR products from the same library were pooled to 30 ng of DNA per sample and concentrated

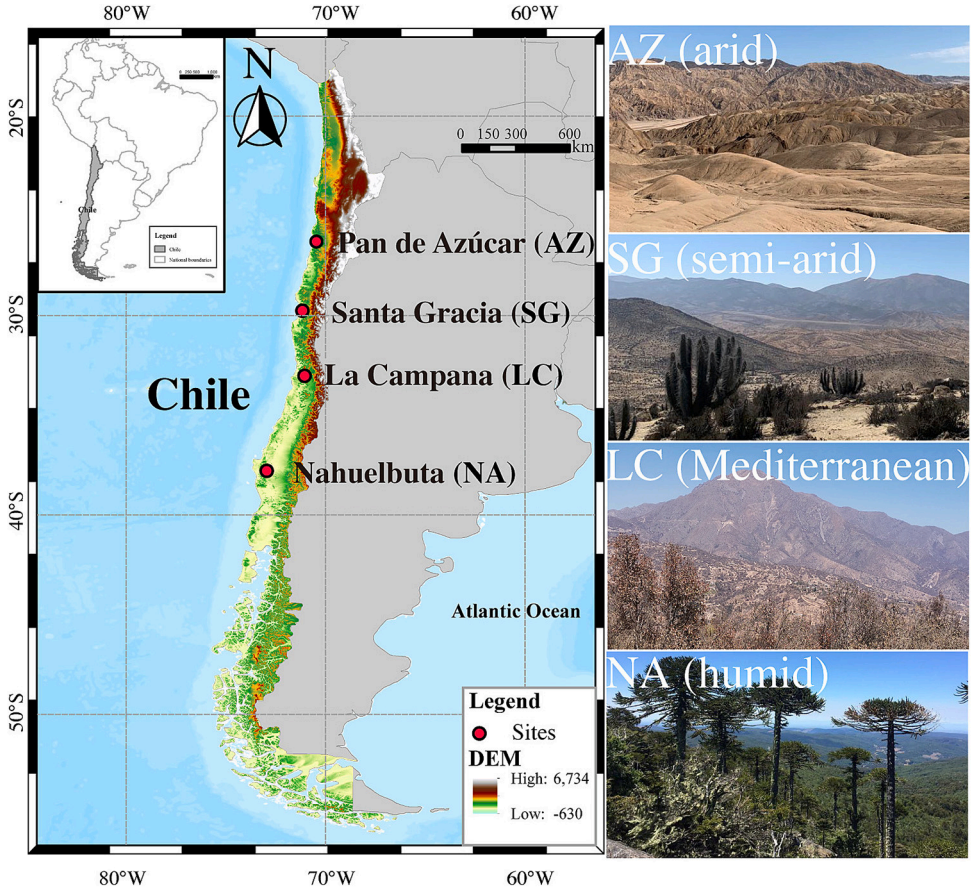

Fig. 1. Site locations are depicted on a digital elevation model (DEM) base map, illustrating characteristics from north to south across the arid Pan de Azúcar (AZ), the semi-arid Santa Gracia (SG), the Mediterranean La Campana (LC), and the humid Nahuelbuta (NA).

to 20–30 μl using a vacuum concentrator (Eppendorf AG, Hamburg, Germany). Three libraries were sent for paired-end sequencing (2 × 300 bp) on an Illumina MiSeq Sequencer (Eurofins Genomics, Konstanz, Germany).

2.4. Soil geochemical analysis

Total carbon (C) and Nitrogen (N) were determined via Dumas combustion using a CHNS analyzer (SERCON© EA, Crewe CW16JT, United Kingdom). Samples were dried at 105 °C and ground using a steel ball mill (Spex Certiprep 8000 M©, Metuchen, NJ, USA). Extractable concentrations of iron (Fe), aluminum (Al), silicon (Si), and manganese (Mn) were determined using ammonium oxalate (poorly crystalline forms, Fe_{ox}, Si_{ox}, Mn_{ox}, and Al_{ox}), sodium pyrophosphate (organically bound forms, Fe_p, Mn_p, and Al_p), and citrate dithionite (Fe_d, Mn_d, and Al_d) extractants, following standard procedures by Burt and Shang (Burt, 2004; Shang and Zelazny, 2008). pH was measured according to Thomas (Thomas, 1996). Available Nitrate Nitrogen (NO_3-N) and Ammonium Nitrogen (NH_4-N) were determined following Miranda et al. (Miranda et al., 2001). Total phosphorus (P_t) and inorganic phosphorus (P_i) were determined using the NaOH and Na_2EDTA extraction, followed by $K_2S_2O_8$ and H_2SO_4 digestion as described by Bowman and Mior (Bowman and Moir, 1993) and Carter and Gregorich (Carter and Gregorich, 2007). Organic phosphorus (P_o) was calculated as the difference between P_t and P_i. All phosphorus fractions were determined colorimetrically using the standard blue ascorbic acid method with a Shimadzu UV-mini 1240 spectrophotometer (Watanabe and Olsen, 1965).

2.5. Data analysis

2.5.1. Processing 16S rRNA gene amplicon data

Paired-end sequencing raw reads were demultiplexed, quality-checked, and trimmed using Cutadapt v3.5 (Magoč and Salzberg, 2011). Reads with low-quality bases (below q20) were excluded. The DADA2 v1.20.0 package (Callahan et al., 2016) was used to fix errors, merge reads, and assign taxonomy, resulting in an amplicon sequence variant (ASV) table using the pooling approach. Non-default parameters were utilized for the *FilterAndTrim* function (truncLen = 240/200, minLen = 200, maxN = 0, maxEE = 2.2, truncQ = 2, rm.phix = TRUE) and the *dada* function (pool = TRUE). The SILVA database v138 (Quast et al., 2013) was used for taxonomic assignment. In order to generate the final ASV table, we excluded singleton mitochondrial and chloroplast ASVs, and ASVs abundant in the negative control (NC). All ASVs in each sample were rarefied to 9435 reads using the R package rtk v0.2.6.1 (Saary et al., 2017) after excluding control samples (NC, PC) and non-bacterial ASVs.

2.5.2. Statistics

We used the DEM dataset from Google Earth Engine (Gorelick et al., 2017) and ArcGIS to visualize the location map. For analyzing and visualizing the community and geochemical data, we used packages and functions in R v4.1.3 (R Core Team, 2022) and Rstudio v1.4.1106 (RStudio Team, 2021). We used tidyverse v1.3.1 to clean and organize the data before conducting further analyses using additional packages and functions (Wickham et al., 2019). Alpha diversity analysis was performed based on the rarefied ASV table and was calculated using vegan v2.6.2 (Oksanen et al., 2022). Permutational multivariate analysis of variance (PERMANOVA), non-metric multidimensional scaling (NMDS) analysis, and distance-based redundancy analysis (dbRDA) were performed with functions *adonis2*, *metaMDS*, and *dbrda*, respectively, in vegan v2.6.2 (Oksanen et al., 2022). Correlations were calculated using the *rcorr* function in Hmisc v4.6.0 package (Harrell Jr, 2021). All physicochemical parameters were tested using the *vif.cca* function, and those with strong covariance (vif > 10) were removed before performing dbRDA. In addition, we used the Bray Curtis distance for NMDS, dbRDA, PERMANOVA, and the heatmap cluster. We used ggplot2 v3.3.6 (Wickham, 2016), pheatmap v1.0.12 (Kolde, 2019), corrplot v0.92 (Wei and Simko, 2021), and patchwork v1.1.1 (Pedersen, 2020) to visualize the data.

To understand how microbial communities adapt to environments, we categorized organisms into "generalists" and "specialists." Generalists thrive in diverse environments by utilizing various resources, while specialists prosper in restricted conditions with limited diets (Székely and Langenheder, 2014; Xu et al., 2021). We analyzed the distribution and abundance of generalists and specialists across sites. ASVs present in over 75 % of the samples and with a high relative abundance (> 0.1 %) across all sites were classified as habitat generalists. During the indicator value analysis (IndVal), we deliberately excluded rare taxa (≤ 0.01 %) to evaluate habitat specialization. The IndVal analysis calculated ASV fidelity and relative abundance within a specific site using the "*indval*" function from the labdsv package (Roberts, 2023). ASVs were considered good indicators of site specialization if they had an IndVal >0.8 and a *p*-value <0.05.

We used weighted correlation network analysis (WGCNA) (Langfelder and Horvath, 2008) to explore co-occurrence modules within the living bacterial community, avoiding misleading correlations between past and present members. Only prevalent taxa were considered; rare and low-abundance ASVs (relative abundance <0.05 % and mean relative abundance <0.02 % across sites) were excluded. Based on scale-free topology criteria, a soft-thresholding power parameter was chosen for the adjacency matrix construction and was utilized for hierarchical clustering, module detection, and co-occurrence network creation. Additionally, we assessed module–trait relationships to explore associations between module membership, sites, and environmental factors.

Co-occurrence network analysis investigated interactions within living bacterial communities across the four study sites. We created a topological overlap matrix (TOM) based on an adjacency matrix determined by a soft-thresholding power parameter. Using this matrix, a reliable and robust co-occurrence network was constructed. The networks were visualized with nodes representing individual taxa and edges indicating significant topological similarity. Visualization and network feature computation were performed using the ggraph and igraph packages (Csardi et al., 2006; Pedersen, 2022).

3. Results

3.1. Sequencing results and ASV identification

Sequencing of 353 samples (320 soil samples and 33 controls) yielded 57,879,300 raw reads. After demultiplexing, filtering, denoising, merging reads, and removing chimeras, 288 samples with 21,502,666 high-quality reads were suitable for analysis. Of these, 97.3 % (20,923,220 reads) were bacteria, and 2.7 % (573,861 reads) were archaea. Classification identified 60,284 unique ASVs, with bacteria comprising 97.6 % (58,822 ASVs). Since the study focused on bacterial communities, archaeal reads were not processed further.

3.2. The physicochemical properties of the soils

The soil physicochemical properties – including pH, conductivity, soil moisture, Al_p, Si_{ox}, and Mn_{ox} – exhibited significant differences between sites (Fig. S1). Soil moisture, Si_{ox}, Mn_{ox}, Mn_p, and Mn_d increased from arid to humid sites while pH decreased. The lowest Fe_{ox}, Al_{ox}, Si_{ox}, and Mn_{ox} were at AZ and the highest at NA. SG had notably higher conductivity than other sites. NA exhibited significantly higher soil moisture, Fe_{ox}, Al_{ox}, Si_{ox}, Mn_{ox}, total C, N, and P_i, but lower pH and conductivity than other sites. The correlation heatmap revealed a negative correlation between depth and various properties, including C, N, soil moisture, and multiple extractable Fe, Al, Si, and Mn (Fig. S2). C, N, Al, Fe, and Mn concentrations decreased with depth, especially in the humid NA region. Furthermore, deeper soil layers had higher soil moisture (Fig. S1).

3.3. Bacterial community distributed along the climate gradient

NMDS analysis based on ASV relative abundance revealed significant differences in community composition between sites (stress = 0.1847) (Fig. 2a). AZ and NA sites were distinctly separated from LC and SG sites. PERMANOVA results indicated that site, depth, and DNA pools significantly influenced community variations, with the site having the strongest effect ($R^2 = 0.191$, $p < 0.001$), followed by depth ($R^2 = 0.042$, $p < 0.001$) and DNA pools ($R^2 = 0.012$, $p < 0.001$).

A heatmap of the top 20 genera across sites and DNA pools revealed

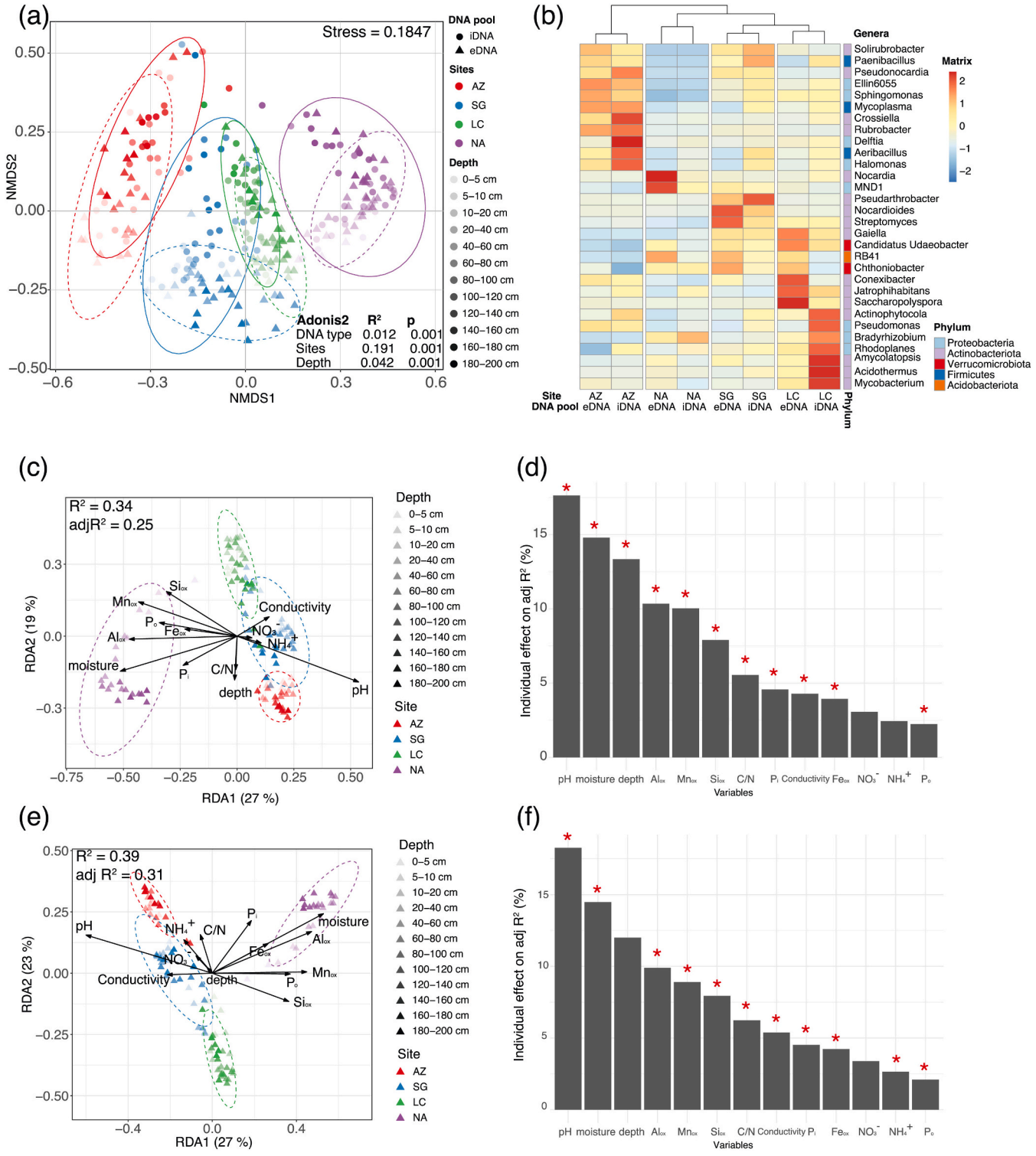

Fig. 2. Analyses of bacterial community structures across sites.
Non-metric multidimensional scaling (NMDS) indicating the similarity of bacterial community structures between sites and DNA at the ASV level (a); heatmap based on the similarity of the distribution of the 30 most abundant genera (b); distance-based (Bray–Curtis) redundancy analysis (dbRDA) indicating the relationships between environmental variables and the bacterial community in the iDNA pool (c) and the eDNA pool (e); hierarchical and variation partitioning for the adjusted R^2 of the dbRDA for the iDNA pool (d) and the eDNA pool (f). Parameters with significant effects are marked with * in the dbRDA and the partitioning plots.

that the iDNA and eDNA community pools within the same site exhibited more remarkable similarity compared with communities from the same DNA pool across different sites (Fig. 2b). This supports the NMDS analysis emphasizing the site as the primary driver of community divergence. The AZ site's community composition differed significantly from other sites, while LC and SG sites displayed high similarity (Fig. 2b).

The dbRDA analysis revealed that physicochemical properties explained more variance in the eDNA pool ($R^2 = 0.31$) than in the iDNA pool ($R^2 = 0.25$) (Fig. 2c, e). Bacterial communities at AZ and SG clustered along the increasing pH axis, indicating a preference for alkaline conditions. In contrast, the NA community aggregated along the axis of increasing soil moisture and higher concentrations of extractable Fe, Al, Si, and Mn, suggesting adaptation to higher moisture and these elements (Fig. 2c, e).

The bar plot from hierarchical and variation partitioning of the adjusted R^2 of dbRDA reconfirmed that pH and soil moisture were the predominant factors influencing bacterial community variations across all sites (Fig. 2d, f). Soil depth substantially affected the iDNA community but not the eDNA community, indicating that the iDNA community was more sensitive to depth changes (Fig. 2c–f). Bray–Curtis dissimilarity analysis highlighted the community composition similarities across depths for both DNA pools (Fig. S3), with significantly higher distances among different depth layers in the iDNA pool, confirming that depth had a stronger influence on the iDNA community (Fig. S3).

3.4. Bacterial community alpha diversity and ASVs distribution

The Shannon and Simpson indices of the eDNA community were significantly higher than those of the iDNA communities for all sites except SG (Fig. 3) and showed a negative correlation with depth (Fig. S4a). In the iDNA community, SG and LC had higher Shannon indices than AZ and NA, while SG and LC had higher Simpson indices than AZ, and AZ had higher Simpson indices than NA (Fig. 3). For the eDNA community, LC had higher Shannon and Simpson indices than other sites (Fig. 3). Generally, diversity showed a unimodal relationship with climatic gradients, with lower diversity at arid and humid regions compared to semi-arid and Mediterranean sites. PERMANOVA analysis showed that soil depth, the sites, and DNA pools significantly influenced bacterial alpha diversity, with depth having the most significant impact (Fig. S4b). ASV distribution analysis showed a higher proportion of unique ASVs in the eDNA pool, particularly in soil layers below 100 cm (Fig. S5).

The separation of iDNA from eDNA revealed distinct differences between the two pools, with varying proportions of unique and shared ASVs (Fig. S5). In the iDNA pool, unique ASVs ranged from 12 % to 36 %, while in the eDNA pool, this ranged from 17 % to 73 %. Shared ASVs ranged from 14 % to 42 %. Notably, the eDNA pool had a significantly higher proportion of unique ASVs in most samples (90 %) than the iDNA pool. However, in some surface soil samples from SG and LC, the unique iDNA proportion exceeded that of the eDNA. As soil depth increased, the proportion of shared and iDNA-unique ASVs slightly decreased, whereas eDNA-unique ASVs significantly increased (Fig. S5).

3.5. Differences in bacterial community structure between eDNA and iDNA pools

The structural differences between the two DNA pools were reflected in the relative abundance of bacterial communities (Fig. 4). Across all study sites and soil depths, the bacterial community composition differed significantly between the iDNA and eDNA pools. For example, at the NA site, the community was dominated by Chloroflexi and Acidobacteriota. The relative abundance of the Chloroflexi phylum was notably higher in the iDNA pools than in the eDNA pools, particularly at lower and middle depths. At other sites, Actinobacteriota and Proteobacteria were prevalent at varying depths, with the Proteobacteria phylum being significantly more abundant in the iDNA pool at both SG and LC. Despite differences in community composition between the two pools, similar trends in community structure and relative abundance with depth were observed in both DNA pools across most sites. Moreover, despite the substantial differences in community composition between the two pools, similar trends in community structure and relative abundance with depth were observed in both DNA pools across most sites. For instance, Actinobacteriota first decreased and then increased with depth at AZ and NA, while their abundance increased steadily with depth at SG.

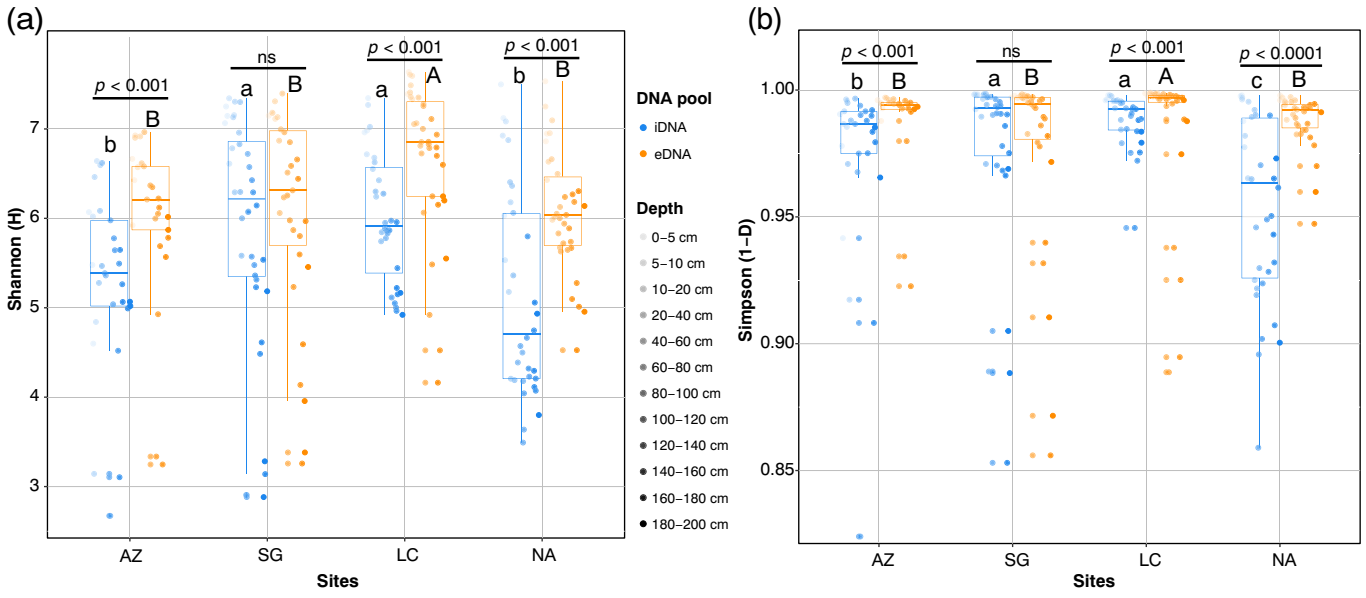

Fig. 3. Variations in alpha diversity indices and ASV distributions according to sites, DNA pools, and depth.
The Shannon (a) and Simpson (b) diversity indices between sites and DNA pools (iDNA: blue; eDNA: orange). Transparency represents depth. The asterisk represents significant differences between DNA pools. Lowercase letters represent significant differences between sites in the iDNA community, and capital letters represent significant differences between sites in the eDNA community.

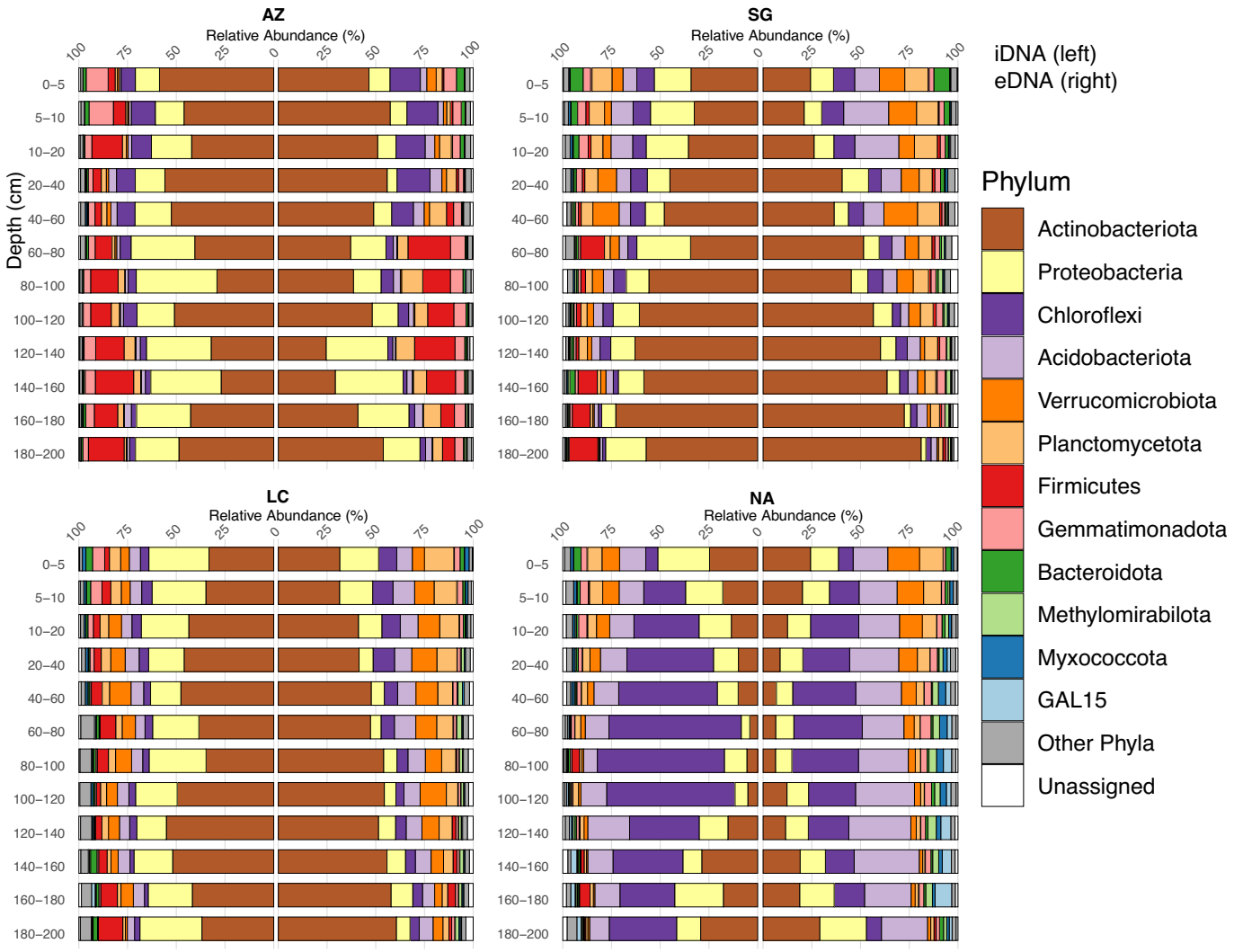

Fig. 4. Relative abundance of dominant microbial phyla in the iDNA and eDNA pools at varying soil depths across distinct climatic regions. The bar diagrams illustrate the microbial community structure in different climatic zones as well as changes in the relative abundance of key phyla with depth in the eDNA and iDNA pools.

A total of 56 bacterial phyla were identified in both DNA pools, with Actinobacteriota (38.18 %), Proteobacteria (15.36 %), Chloroflexi (12.94 %), Acidobacteriota (9.39 %), and Verrucomicrobiota (5.00 %) being the dominant phyla. The abundances of these phyla varied across sites, soil depths, and DNA pools (Figs. 4, 5). Actinobacteria were highly abundant across all sites and DNA pools, particularly in the surface layer (0–40 cm) of AZ and the deep layer (120–200 cm) of SG (Figs. 5, S6, 7). The relative abundance of the genus *Rubrobacter* decreased from north to south. Acidobacteriota were primarily found in the middle and deep layers of NA (Figs. S6, 7). Verrucomicrobiota was mainly observed at the surface (0–40 cm) and intermediate (40–120 cm) layers of NA, SG, and LC (Figs. 5, S6, 7). Proteobacteria exhibited higher abundance within the iDNA pool, particularly in intermediate and deep depths. At the same time, Chloroflexi showed higher abundances in the iDNA pool of NA, particularly in intermediate layers (40–120 cm) (Figs. S6, 7).

The 16S rRNA gene copy numbers in the eDNA pool were significantly higher than in the iDNA pool in nearly all samples, indicating a higher abundance or accumulation of dead bacteria than living bacteria (Fig. S8). The highest bacterial gene copy numbers were observed at SG, LC, and NA, ranging from 8 to 10 $\times$ 10^8 gene copies g^{-1} soil (Fig. S8). In contrast, AZ had significantly lower gene copy numbers, about 10–15 % of those found at other sites. Gene copy numbers also decreased 100-fold with increasing depth. At the arid site (AZ), higher gene copy numbers, particularly in the iDNA pool, were found in the deeper soil layer (10–20 cm) rather than at surface depths (0–5 and 5–10 cm) (Fig. S8), suggesting that the surface soil at AZ was less suitable for bacterial survival than the subsurface layer.

We observed distinct patterns in the bacterial communities of the iDNA pool along the transect (Fig. S8). The humid site exhibited the highest bacterial abundance, while the arid site showed considerably lower abundance, especially in the uppermost 5 cm of soil. The semi-arid and Mediterranean sites had higher bacterial abundances than the arid sites, with slight differences. In contrast, the eDNA pool revealed notable differences along the transect, with the most significant distinctions under arid conditions (Fig. S8). Minor variations were observed in semi-arid, Mediterranean, and humid conditions, particularly up to 60 cm deep (Fig. S8).

3.6. *Bacterial generalists and specialists along the climate gradient*

The analysis of the bacterial iDNA pool in the surface layer (0–40 cm) revealed both generalist and specialist bacteria. Across the surface soil (0–40 cm), we identified 23 generalist taxa, highlighting their adaptability to the studied ecosystems (Fig. 6a). These generalist taxa belonged to 5 phyla: Actinobacteria, Proteobacteria, Acidobacteriota, Chloroflexi, and Firmicutes. While present at all sites, their abundance

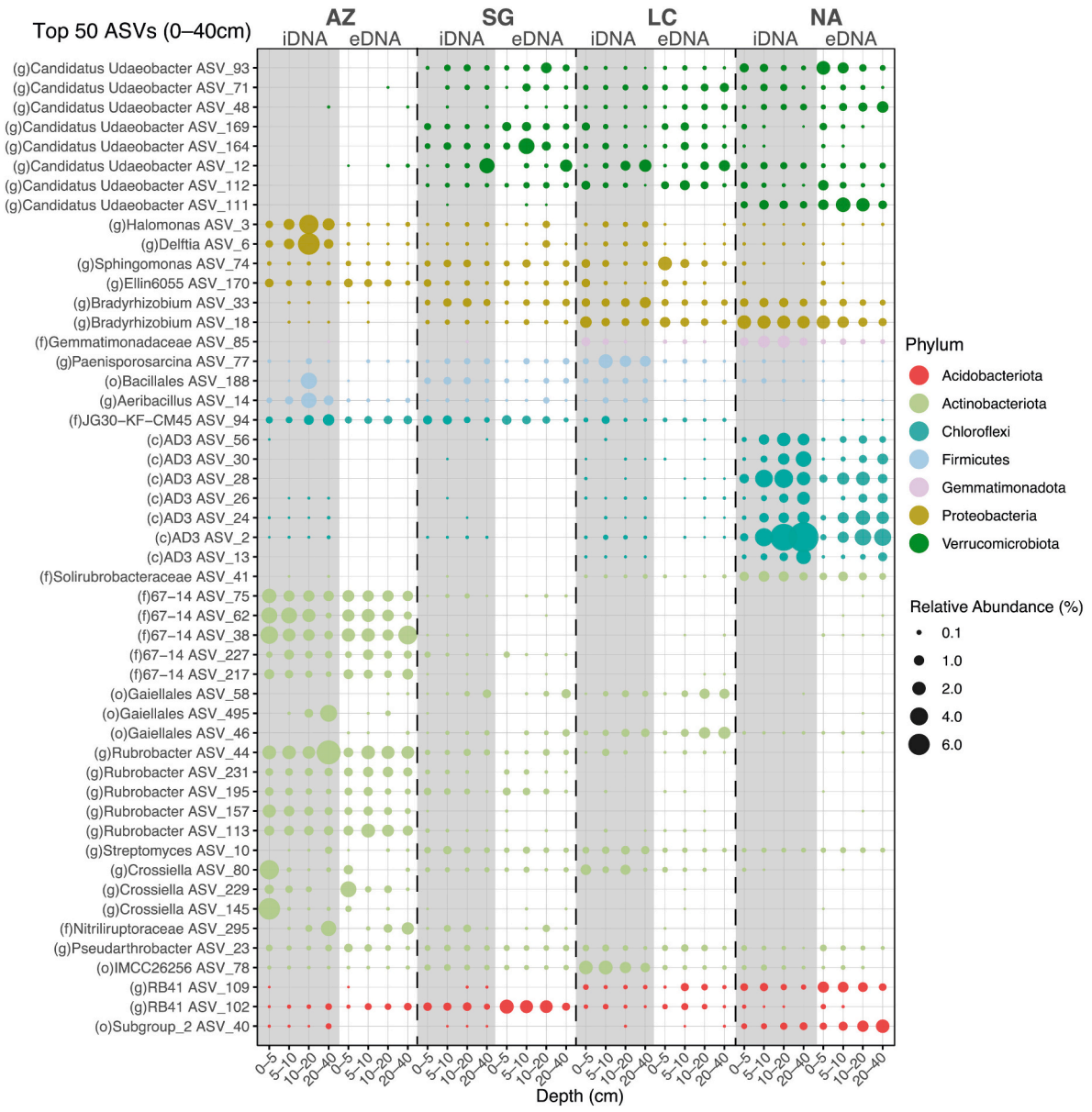

Fig. 5. Bubble plot depicting the distribution and relative abundances of the top 50 bacterial ASVs in separate DNA pools (iDNA is represented with a gray background; eDNA is represented with a white background) at 0–40 cm. Each filled circle represents the presence of a particular ASV, with its size being proportional to its relative abundance. Taxonomic classifications are provided at the levels of phylum (p), class (c), order (o), family (f), and genus (g).

varied across specific sites. For instance, the *Bradyrhizobium* genus increased north to south, while the taxa of *Halomonas*, *Delftia*, and *Aeribacillus* genera were predominant at AZ. SG had a notable presence of the genus *RB41* and the order Bacillales, whereas LC had a higher abundance of the order IMMC26256 and the genus *Paenisporosarcina*. The class AD3 exhibited considerable abundance at NA, with ASVs showing an increasing trend in the subsurface layers (Fig. 6a).

In the indicator value analysis (Table S2), we identified ASVs from 7 phyla as bacterial specialists in the iDNA pool: Acidobacteriota, Actinobacteriota, Chloroflexi, Firmicutes, Gemmatimonadota, Proteobacteria, and Verrucomicrobiota (Fig. 6b). A total of 36 specialists were identified across sites, with AZ having the most (14), followed by NA (11), LC (10), and SG (1). Actinobacteriota was the most dominant phylum among the specialists and was present at all sites. For example, AZ specialists included ASVs from the genera *Rubrobacter* and *Crossiella*, the families 67–14, and the class Alphaproteobacteria. SG had a sole specialist identified as the order Rhizobiales. At LC, specialists consisted of ASVs from the genus *Paenisporosarcina* and the orders Elsterales, Gaiellales, and IMCC26256. NA specialists included ASVs from the genera *Candidatus* Udaeobacter, *Burkholderia–Caballeronia–Parabu rkholderia*, genera *RB41*, order Vicinamibacterales, families Xanthobacteraceae, and Solirubrobacteraceae, and the AD3 class (Fig. 6b).

3.7. WGCNA and co-occurrence network analysis

WGCNA identified 17 distinct co-occurrence modules within the bacterial community, consisting of a unique set of taxa with strong co-occurrence patterns. 696 ASVs were assigned to these modules, highlighting the community's diverse composition. Nevertheless, 16 ASVs were unassigned and categorized as the "gray" module. Module sizes ranged from 20 to 72 ASVs, which reflected variations in complexity and organization. Detailed module composition can be found in Supplementary Table S3.

We found distinct taxonomic compositions within each module, with specific taxa showing higher abundance and stronger co-occurrence. For example, Modules 1, 3–8, and 10–17 were dominated by members of the

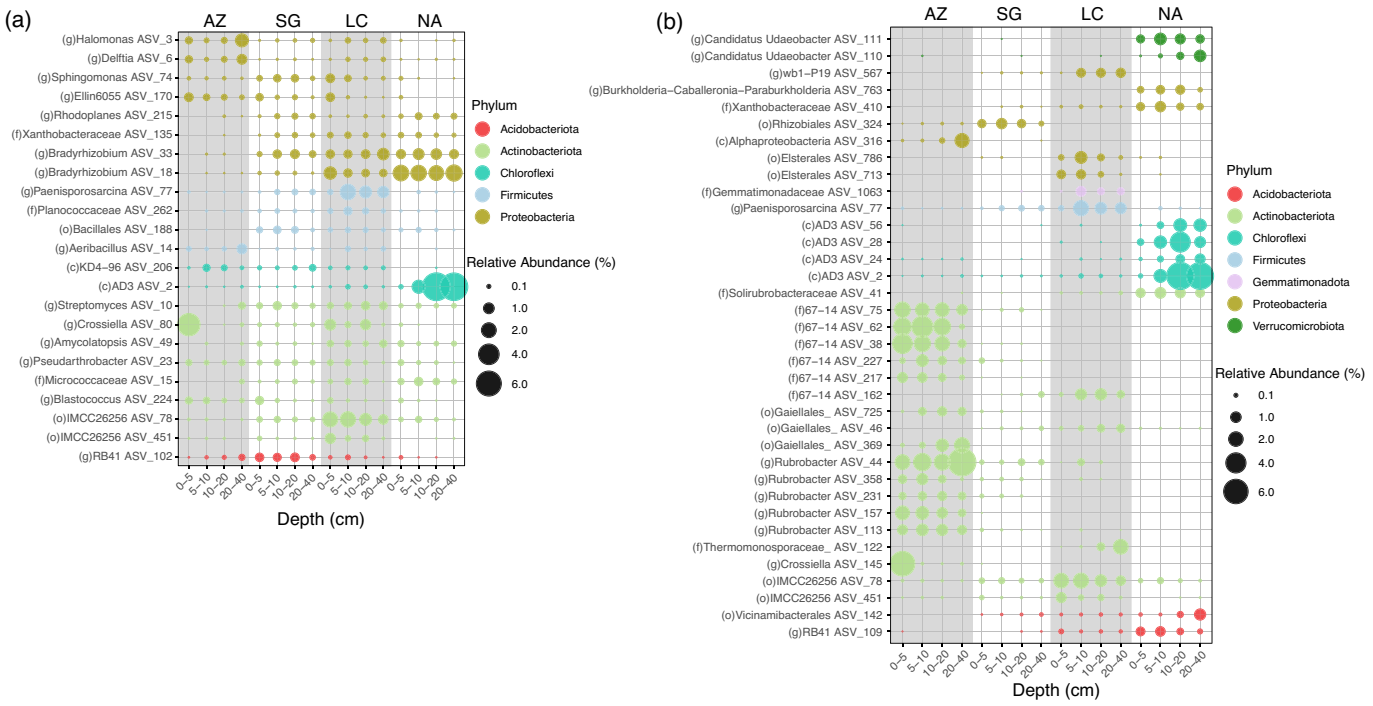

Fig. 6. Bubble plot depicting the distribution and relative abundances of the generalists (a) and specialists (b) at four sites in the iDNA pool. Each filled circle represents the presence of a particular ASV, with the size of the circle being proportional to the relative abundance of the ASV. Taxonomic classifications are provided at the levels of phylum (p), class (c), order (o), family (f), and genus (g).

phyla Actinobacteria and Proteobacteria, especially the orders Gaiellales, Solirubrobacterales, Pseudonocardiales, Streptosporangiales, Rubrobacterales, and Frankiales. Modules 2 and 9 were dominated by the phyla Chloroflexi and Acidobacteriota, especially the class AD3 and the order Vicinamibacterales. Hub taxa within the modules, highly connected and influential in the network, play crucial roles in community dynamics and ecosystem processes. The hub taxa included members of the phyla Actinobacteriota, Proteobacteria, Planctomycetota, Acidobacteriota, and Verrucomicrobiota (Table S4).

To understand the functional relevance of these modules, we

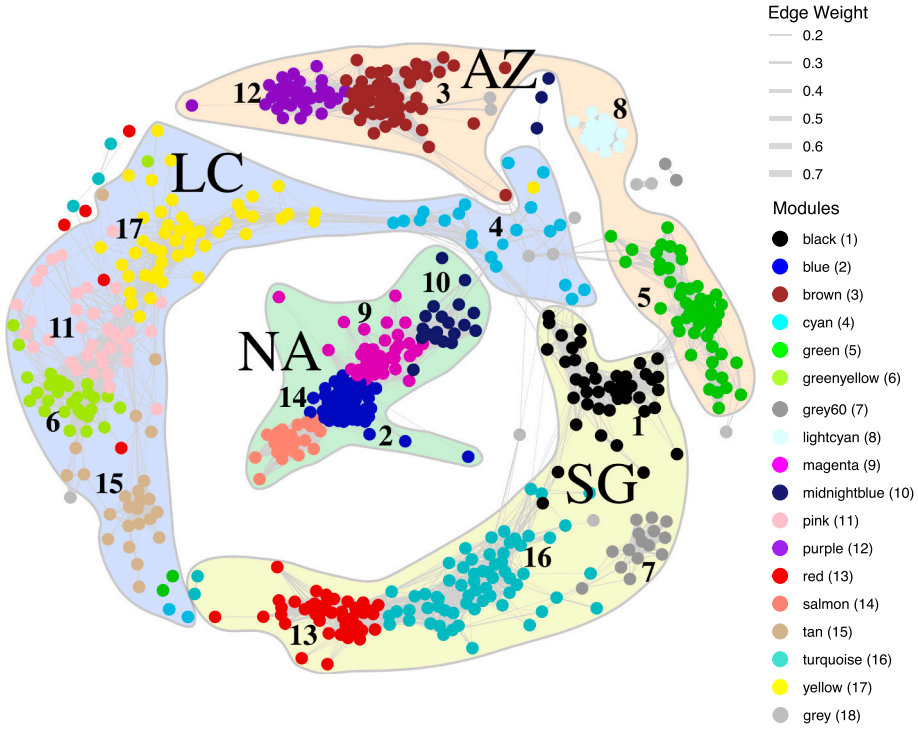

Fig. 7. Co-occurrence network of bacterial communities at four sites along the Chilean Coastal Cordillera: Pan de Azúcar (AZ), Santa Gracia (SG), La Campana (LC), and Nahuelbuta (NA). Nodes represent ASVs and are color-coded based on their module membership. In order to reduce complexity, only edges with topological similarity higher than 0.1 are displayed. The different background colors represent the module–site relationship results.

conducted a module–trait relationship analysis exploring associations between module features and environmental factors. Interestingly, significant correlations between specific modules and key environmental variables suggested potential functional roles of the corresponding taxa in response to environmental conditions (Fig. S9). Several modules displayed significant associations with multiple environmental factors, highlighting their multifunctional roles in the microbial community. For instance, Modules 2 and 9 displayed positive correlations with soil moisture, N, C, Fe_{ox}, Fe_{ox}/Fe_d, Fe_p, Al_{ox}, Al_p, Si_{ox}, NH_4-N, P_i, Mn_d, Mn_{ox}, and Mn_p, which suggested a coordinated response of the modules to these variables. Conversely, Modules 2, 9, 10, and 14 negatively correlated with pH (Fig. S9), revealing adaptation to acidic environments.

Our analysis explored the relationship between module features, study sites, and soil depths, revealing the prevalence of module members at specific locations. Significant associations were observed between modules and study sites. Modules 3, 5, 8, and 12 were strongly associated with the AZ site (Figs. 7, S10). Modules 1, 7, 13, and 16 were predominantly related to the SG site, while Modules 4, 6, 11, 15, and 17 were strongly associated with the LC site. Modules 2, 9, 10, and 14 were primarily linked to the NA site, highlighting site-specific patterns within the bacterial community. Modules 1 and 4 were notably associated with the 0–5 cm and 5–10 cm depth ranges, suggesting the preferential abundance and co-occurrence within these layers. Modules 7 and 12 exhibited a pronounced association with deep soil, particularly at the 160–180 cm depth (Fig. S11). This suggests that these module communities may be adapted to deep underground environments with low organic matter.

Following the removal of self-loops and weak relationships, the co-occurrence network analysis unveiled a bacterial network with 647 nodes and 8508 edges (Fig. 7). The network exhibited a high average clustering coefficient of 0.74, thereby indicating dense interconnectivity among taxa. The relatively short average path length of 0.89 suggested efficient co-occurrence patterns. Moreover, the network diameter was 2.17, representing the maximum steps required to traverse the network. The network, built on WGCNA–identified modules, displayed a distinct clustering pattern that correlated with the site associations, highlighting site-specific module clustering (Figs. 7, S10). More features are detailed in Supplementary Tables S5 and S6.

4. Discussion

4.1. Improved resolution of microbial community structure through DNA separation

The DNA separation method used in this study differentiated between DNA from intact living cells (iDNA) and dead DNA preserved in soils (eDNA). The eDNA constituted most of the total DNA in our samples – a finding supported by existing literature (Ceccherini et al., 2009). The prevalence of eDNA can bias microbial community analyses based on total DNA (tDNA). The DNA separation method allowed us to specifically focus on the living microbial community (iDNA pool), thereby eliminating the bias introduced by the prevalence of eDNA in environments such as the Atacama Desert, where microbial communities exhibited intermittent activity and low metabolic rates (Schulze-Makuch et al., 2018).

The eDNA pool included diverse DNA sources from cell lysis, active secretion by living cells, and the external input of biogenic matter (Ibáñez de Aldecoa et al., 2017). Unlike free eDNA, which degrades rapidly, DNA adsorbed onto minerals can persist for extended periods, even geological timescales (Pedersen et al., 2021). Clay minerals, for instance, facilitate DNA preservation through adsorption (Ogram et al., 1987). Adsorbed DNA can move through soil sedimentation and leaching (Haile et al., 2007), potentially reducing microbial community variability between soil depths. Consequently, accurate estimations of present biodiversity necessitate distinguishing between iDNA and eDNA (Thomsen and Willerslev, 2015).

Our results showed that the eDNA pool was significantly more abundant and diverse and had more unique species than the iDNA pool, especially in deeper soils (Figs. 3, S5, 8). These results were attributed to the accumulation of eDNA over time, which was more favorable for eDNA preservation in environments with low oxygen and low organic matter in deeper soil layers (Morrissey et al., 2015) (Torti et al., 2015; Y. Li et al., 2021).

While both DNA pools exhibited responses to various climate conditions along the transect, their reactions conveyed distinct ecological implications. First, the eDNA abundance in surface soil at SG, LC, and NA was comparable and consistent with prior research (Bernhard et al., 2018). In contrast, iDNA abundance at the humid NA site was significantly higher than at other sites (Fig. S8). This supports the notion that iDNA abundance is particularly sensitive to changes in climate. In addition, the iDNA bacterial community diversity responded rapidly to increased soil moisture, with SG showing significantly higher diversity than AZ. In contrast, significant eDNA differences were only observed at LC (Fig. 3a). More specifically, the trend in eDNA community diversity mirrored the trend in total DNA from AZ to NA, as reported by Bernhard et al. (Bernhard et al., 2018). This alignment was attributed to two key factors: First, eDNA constitutes a substantial portion of environmental DNA (Ceccherini et al., 2009) compared with iDNA. Consequently, changes in the eDNA community likely reflect overall total DNA trends. Second, eDNA accumulates genetic material over time, encompassing DNA from various sources, including living organisms and remnants of dead cells (Carini et al., 2016; Bairoliya et al., 2022).

Furthermore, we identified three distinct patterns of species abundance in both DNA pools (Figs. 5, S6, S7): First, certain species showed significant abundance in the iDNA pool, indicating their adaptation to the prevailing conditions. For example, the genus *Halomonas*, known for its saline habitat tolerance and efficient oxygen metabolism, was abundant at the arid AZ site (Ventosa et al., 2021). Similarly, the genus *Delftia* –adapted to low organic environments – was prevalent in the AZ iDNA pool (Bhat et al., 2022) suggesting its active adaptation to arid, subterranean depths with limited organic matter and water availability. The enrichment of AD3 in the iDNA pool at the acidic NA is consistent with the prevalent adaptation of AD3 to various acidic environments (Mesa et al., 2017).

Second, Nocardia species – influenced by soil moisture, pH, temperature, and organic matter – were enriched in the deeper soil layers at the humid NA, as observed in the eDNA pool (Fig. S7). Although resistant forms – such as Nocardia spores – are typically associated with the iDNA pool due to their long-term survival mechanisms (Sharma et al., 2016), their abundance in the eDNA pool could indicate their historical prevalence. The eDNA likely originated from degraded cell fragments once part of the active microbial community, indicating a historical ecological footprint.

Finally, maintaining consistent relative proportions, certain bacteria exhibited similar abundances in both iDNA and eDNA pools. This observation suggests a continual replenishment of the eDNA pool by the biomass turnover of living cells (Levy-Booth et al., 2007) and implies adaptation to past and present soil environments. The iDNA results reveal distinct differences in bacterial abundances across various climate conditions, providing new insights into the dynamics of microbial populations across multiple climate settings. This novel finding indicates that iDNA could serve as a valuable indicator for tracking short and medium-term climate changes, particularly in low-biomass soils transitioning between arid, semi-arid, and humid conditions.

Overall, employing the DNA separation method allowed us to analyze dead soil microbial communities, demonstrating its efficacy, especially in low-biomass habitats and deeper subsurface where conventional metagenomics and transcriptomics approaches may be less effective or impossible. This method provided insights into microbial communities in deep soil profiles, often overlooked in favor of surface studies.

4.2. Discovery of climate-driven patterns of microbial diversity and adaptive communities via the separation method

Building upon the enhanced resolution from DNA separation, our iDNA-based analyses revealed variations in living and potentially active bacterial communities across the climate transect. The bacterial community at each site was shaped by environmental factors such as pH, soil moisture, organic matter content, and extractable mineral content (Fig. 2). Microbial communities adapted as habitat generalists or specialists in response to these gradients. Generalists exhibited broad environmental tolerance and thrived in various habitats, while the specialists possessed a narrower environmental range and were often restricted to specific niches (Székely and Langenheder, 2014; Xu et al., 2021).

In our study, the generalists belonged to the dominant phyla that prevailed across all sites: namely Actinobacteria, Proteobacteria, Acidobacteriota, Chloroflexi, and Firmicutes (Fig. 6a). This indicates their adaptability to diverse environments, including extreme conditions. Generalist taxa from Actinobacteria contributed to the decomposing and recycling of carbon, nitrogen, phosphorus, potassium, and other essential elements in the soil (Goodfellow and Williams, 1983; Holmalahti et al., 1994; Hill et al., 2011). The saprophytic nature of these taxa led to the production of various extracellular hydrolytic enzymes that were capable of breaking down complex organic compounds, such as lignin, cellulose, chitin, and other plant and animal polymers (Eisenlord and Zak, 2010). Proteobacteria and Actinobacteria are recognized for their physiological and metabolic diversity, with adaptive strategies such as versatile energy metabolism, the ability to utilize various carbon sources, and diverse stress response mechanisms (Spain et al., 2009; Schulze-Makuch et al., 2018). These attributes allow the two taxa to thrive in diverse conditions. While the ecological role of Acidobacteriota RB41, recognized as a generalist, remains incompletely elucidated, recent studies suggest it significantly influences the soil carbon cycle by aiding in organic matter breakdown and stabilizing the soil carbon pool (Stone et al., 2021). The variability in abundance of these generalists across specific sites could be attributed to the site-specific environmental conditions and ecological niches that influence the generalists' populations.

Specialists, in contrast, were the indicators of the climatic transition from arid to humid conditions along the transect. They were highly adapted to local environmental conditions. For example, the genus *Rubrobacter*, known for its exceptional radiation resistance and ability to thrive in arid soils (Holmes et al., 2000; Suzuki, 2015), dominated the AZ regions (Fig. 6b). At the humid NA site, the Xanthobacteraceae family was abundant and displayed capabilities in nitrogen fixation (Oren, 2014), plant associations (da Silva et al., 2002), and organic matter degradation (Wilhelm et al., 2019). The high abundance of Xanthobacteraceae at NA could be attributed to soil pH, the availability of weathered minerals, and abundant carbon resources (Jones, 2015). Moreover, the humid NA site – with its active iron content and low pH – exhibited the highest abundance of Acidobacteriota, known for thriving in iron-rich environments (Dedysh and Oren, 2019; Patzner et al., 2020). Among the specialists at NA, *Candidatus* Udaeobacter –an acidophilic genus – potentially significantly enhanced soil aggregates and promoted stability (Szoboszlay and Tebbe, 2021).

Our study identified several generalist and specialist taxa, also reported by Rodriguez et al. (2022), in the same region using a total DNA approach. Interestingly, other taxa reported in the earlier study were abundant in the eDNA pools in our investigation. This observation highlights the benefit of the separation method in identifying generalist and specialist taxa based on the iDNA pool.

4.3. Depth relationships in light of the DNA separation method

Shifting the focus to depth, our study was the first to employ the e/iDNA separation method to analyze living and potentially active microbial communities in deep soil compartments. In the arid region (AZ), a distinctive trend emerged: The surface layer (0–5 cm) exhibited reduced abundance and diversity – particularly in the iDNA pool – when compared with the 10–20 cm layer (Figs. 3, S8). This difference mirrored the microbial distribution observed in the hyper-arid Atacama Desert, where bacterial abundance was higher at the 20–30 cm depth than at the surface (Schulze-Makuch et al., 2018). The differences may result from harsh surface conditions in arid areas, including extreme drought, intense UV radiation, and significant temperature fluctuations (van Gestel et al., 2013) that inhibit bacterial growth.

Our research underscores the significant role of localized conditions, such as humidity, temperature, and radiation intensity, in shaping microbial communities. These factors, which vary with climate and depth, influence the degradation rate of eDNA and the activity of living microorganisms. Stress conditions, including oxidative stress, radiation exposure, and nutrient deprivation, can damage cells and trigger programmed cell death (Hoeksma et al., 2015; Yang et al., 2019). This is exemplified by the radiation-resistant genus *Rubrobacter*, which negatively correlated with depth (Fig. S12). These findings highlight how localized conditions can influence microbial abundance and distribution (Puche et al., 2021).

Previous research has consistently found a decrease in microbial abundance with increasing soil depth (Bernhard et al., 2018) down to the saprolite layer (Oeser et al., 2018). These studies underscore the pivotal role of soil physicochemical properties, such as organic matter content and plant carbon sources, in shaping microbial diversity and structure at different depths(Ekelund et al., 2001; Huang et al., 2014). Building upon this prior research (Sharrar et al., 2020), our study revealed that soil depth primarily influences alpha diversity. In contrast, the sampling site had a more substantial impact on beta diversity (Fig. 2a). The iDNA communities demonstrated high sensitivity to depth (Fig. 2c, d) due to depth-dependent variations such as UV radiation, organic matter, and soil oxygen content, affecting active bacteria growth (Erich et al., 2012). In contrast, the eDNA pool was insensitive to depth (Fig. 2e, f). We attributed this finding to two key factors: First, the non-metabolic nature of eDNA renders it less responsive to depth-dependent soil parameters, and second, eDNA is more susceptible to leaching from the surface to the subsurface layers (Haile et al., 2007), thereby resulting in similar distribution across depths (Fig. S3). In summary, our pioneering use of the e/iDNA method in deep soil profiles not only distinguished microbial responses with depth but also enhanced our understanding of the impacts of localized conditions on microbial groups. Thus, this novel approach is a superior tool for unraveling the intricate relationships between microbial communities, depth-dependent factors, and the environment.

4.4. Indication of determinism in the formation of the co-occurrence network of the living bacterial community

By bridging insights from climate-driven patterns and depth variations, the WGCNA analysis of the living bacterial community unveiled distinct co-occurrence modules of unique bacterial taxa with solid patterns not visible in tDNA-based analyses.

The identified modules comprised diverse bacterial species (Acidobacteriota, Actinobacteriota, Chloroflexi, Proteobacteria, and Firmicutes) known for their roles in soil formation, development, and ecosystem functioning. For example, Xanthobacteraceae contribute to nitrogen fixation in soil fertility improvement (Yan et al., 2019). Conexibacter – a member of the order Solirubrobacterales – is associated with chemosynthetic CO2 fixation and ferrous–ferric redox reactions, enhancing weathering and micronutrient availability in soils (Sánchez-Marañón et al., 2017; Aanderud et al., 2018; Meier et al., 2019). Moreover, Gemmatimonadetes – adapted to low soil moisture – were linked to phosphorus metabolism (Genderjahn et al., 2018; O'Brien et al., 2019; Garrido-Benavent et al., 2020).

Modules 3, 5, 8, and 12, linked to the arid AZ site, consisted of

diverse taxa, such as Actinobacteriota (Crossiella, Rubrobacter, Gaiellales) and Proteobacteria (Sphingomonas, Rhizobiales). Their presence suggested functional implications for nutrient cycling (Zhang et al., 2022), organic matter decomposition (Tao et al., 2020), and soil formation (Kim et al., 2021). Actinobacteria decompose complex organic compounds, aiding in nutrient mineralization and cycling (Schulze-Makuch et al., 2018). Proteobacteria – especially Sphingomonas and Rhizobiales –degrade pollutants and facilitate plant-microbe interactions (Spain et al., 2009; Schulze-Makuch et al., 2018). Together, these taxa likely synergize, enhancing nutrient cycling, organic matter decomposition, and soil formation, influencing overall ecosystem function and sustainability.

We identified hub taxa that played central roles within their modules, with Actinobacteria being the most common (11 out of 17 hub taxa, Table S4). In contrast, in the humid NA, other taxa emerged as network hubs, including Proteobacteria (1 taxon), Acidobacteriota (1 taxon), Planctomycetota (1 taxon), and Verrucomicrobiota (1 taxon) emerged as pivotal contributors. These taxa are significantly involved in nitrogen fixation (Rahimlou et al., 2021), soil pH regulation (Dyksma and Pester, 2023), and decomposition processes (Kulichevskaya et al., 2019), actively influencing microbial community dynamics in response to the humid environment.

Module–trait relationships revealed significant associations with key environmental factors (Fig. S9). Modules associated with AZ displayed a strong positive correlation with pH and a negative correlation with extractable elemental content, attributed to Actinobacteria's dominance, desiccation resistance traits, and metabolic versatility suited to arid soils such as the Atacama Desert (Schulze-Makuch et al., 2018). Conversely, the humid NA site showed negative correlations with pH and positive correlations with moisture and extractable elemental content, aligning with Actinobacteria, Proteobacteria, and Chloroflexi adaptation to humid environments (Reis et al., 2019). At the semi-arid and Mediterranean sites, less distinct associations with soil properties emerged compared with the arid and humid sites. The Mediterranean site showed associations with plant-available phosphorus, conductivity, and manganese. In contrast, the semi-arid SG site exhibited a similar – albeit weaker – trend to the arid AZ site, thereby indicating bacterial responses to environmental factors.

The soil modules identified in this study suggest potential mutualistic, symbiotic, complementary, and synergistic interactions among bacterial groups, though these interactions remain poorly documented. Actinobacteriota, Proteobacteria, and Firmicutes may engage in mutualistic relationships, with Actinobacteriota decomposing organic matter (Bao et al., 2021), Proteobacteria assisting in nutrient cycling (Karimi et al., 2018; Langwig et al., 2022), and Firmicutes enhancing soil structure formation. Similarly (Q. Li et al., 2021), Acidobacteriota, Chloroflexi, and Actinobacteriota may exhibit complementary interactions in organic matter degradation (Bayer et al., 2018), nutrient cycling, and carbon sequestration (Gonçalves de Chaves et al., 2019). Nonetheless, further research is needed to fully understand these microbial interactions and their significance in soil ecosystems.

In general, deterministic processes that govern community assembly are influenced by environmental variables such as soil pH, moisture, and nutrient availability (Fig. S9). These factors drive composition in soil bacterial communities along the Chilean Coastal Cordillera. The associations between network modules and soil physicochemical properties highlight climate's significant impact on the composition and structure of bacterial communities. Additionally, some modules were enriched in deeper soil layers, which may stem from adaptation to low organic matter and limited oxygen availability (Fig. S11).

The clustering of different modules from the same site in the co-occurrence network indicated specific connections among these modules (Fig. 7), revealing environmental determinism in community formation and leading to interconnected bacterial communities. Specific taxa and their interactions are crucial in shaping the structure of bacterial communities within these ecosystems. These findings from the iDNA pool improve our understanding of soil bacterial community dynamics and underscore the significant influence of climate on microbial community composition and assembly processes.

5. Conclusions

This study employed an innovative DNA separation method to investigate bacterial community dynamics across an extreme climate gradients and soil depths along the Chilean Coastal Cordillera that presented similar granitoid parent materials. By distinguishing between living (iDNA) and dead (eDNA) bacteria, we better understood how climate change and soil depth influence microbial community composition and diversity.

Our findings revealed that the eDNA pool exhibited higher abundance and diversity due to its accumulation over time and correlated strongly with environmental factors. In contrast, the iDNA pool community showed more pronounced responses to climate change, with greater abundance, rapid variation, and significant responses to moisture and other soil parameters. Additionally, the eDNA pool exhibited less depth-dependent variation than the iDNA pool. The iDNA's sensitivity to depth may be explained by its metabolic activity, making it more responsive to depth-dependent parameters, such as moisture and oxygen. At the same time, the leaching-effected eDNA pool showed relatively slight variations between depths. Our results also revealed a distinct microbial transition from arid to humid areas and confirmed the adaptation of soil bacteria's ecosystem-functional traits to their environment. Modules related to climates clustered individually and were influenced by environmental variables in the co-occurrence network, which unveiled a deterministic climate-related pattern among the bacterial communities.

This innovative approach, combined with physicochemical property analysis and network analytical techniques, unveils the complex interactions between microbes and environmental factors. It offers more profound insights into ecosystem functions, demonstrating the iDNA pool could provide valuable information for regional soil microbial studies across different depths.

Funding

This research was supported by the Deutsche Forschungsgemeinschaft (DFG) within the framework of the priority program SPP-1803 "EarthShape: Earth Surface Shaping by Biota" via a grant to Dirk Wagner (WA 1554/17). Xiuling Wang was additionally supported by the China Scholarship Council (201909505013).

CRediT authorship contribution statement

Xiuling Wang: Writing – review & editing, Writing – original draft, Visualization, Validation, Supervision, Software, Resources, Project administration, Methodology, Formal analysis, Data curation, Conceptualization. **Lars Ganzert:** Writing – original draft, Investigation, Conceptualization. **Alexander Bartholomäus:** Visualization, Methodology, Data curation. **Rahma Amen:** Writing – review & editing, Writing – original draft. **Sizhong Yang:** Visualization, Methodology. **Carolina Merino Guzmán:** Investigation. **Francisco Matus:** Investigation. **Maria Fernanda Albornoz:** Investigation. **Felipe Aburto:** Investigation. **Rómulo Oses-Pedraza:** Investigation. **Thomas Friedl:** Conceptualization. **Dirk Wagner:** Writing – review & editing, Writing – original draft, Supervision, Project administration, Investigation, Conceptualization.

Declaration of competing interest

The authors declare that the research was conducted without any commercial or financial relationships that could be construed as a potential conflict of interest.

Data availability

The demultiplexed 16S rRNA sequences were deposited in the European Nucleotide Archive database (Accession Number: PRJEB73502; https://www.ebi.ac.uk/ena/browser/view/PRJEB73502). The sequence data are not publicly available and will be made public after the publication of the present article. The codes used for analysis and visualization in this research project are stored on GitHub (https://github.com/Xiuling-Wang/The-effects-of-climate-and-soil-depth-on-living-and-dead-bacterial-communities).

Acknowledgements

The authors wish to thank Aurele Vuillemin (GFZ: German Research Centre for Geosciences) for his insightful discussions, GaoDu Liang (Dongguan City Construction Planning Design Institute) for his help in making the geographic map, and ZhongYi Hua (Chinese Academy of Chinese Medical Sciences) for his help in data visualization. We also express our deep gratitude to all the colleagues who aided us in the field, especially Kirstin Übernickel (University of Tübingen) and Leandro Paulino (University of Concepción).

Appendix A. Supplementary data

Supplementary data to this article can be found online at https://doi.org/10.1016/j.scitotenv.2024.173846.

References

Aanderud, Z.T., Saurey, S., Ball, B.A., Wall, D.H., Barrett, J.E., Muscarella, M.E., et al., 2018. Stoichiometric shifts in soil C:N:P promote bacterial taxa dominance, maintain biodiversity, and deconstruct community assemblages. Front. Microbiol. 9 https://doi.org/10.3389/fmicb.2018.01401.

Alawi, M., Schneider, B., Kallmeyer, J., 2014. A procedure for separate recovery of extra- and intracellular DNA from a single marine sediment sample. J. Microbiol. Methods 104, 36–42. https://doi.org/10.1016/j.mimet.2014.06.009.

An, S., Mao, Z., Chen, M., Huang, X., Shi, L., Xing, P., et al., 2023. Sunlight irradiation promotes both the chemodiversity of terrestrial DOM and the biodiversity of bacterial community in a subalpine lake. Environ. Res. 227, 115823 https://doi.org/10.1016/j.envres.2023.115823.

Bairoliya, S., Xiang, Koh Zhi, J., and Cao, B., 2022. Extracellular DNA in environmental samples: occurrence, extraction, quantification, and impact on microbial biodiversity assessment. Appl. Environ. Microbiol. 88, e01845-21 https://doi.org/10.1128/aem.01845-21.

Bao, Y., Dolfing, J., Guo, Z., Chen, R., Wu, M., Li, Z., et al., 2021. Important ecophysiological roles of non-dominant Actinobacteria in plant residue decomposition, especially in less fertile soils. Microbiome 9, 84. https://doi.org/10.1186/s40168-021-01032-x.

Bayer, K., Jahn, M.T., Slaby, B.M., Moitinho-Silva, L., Hentschel, U., 2018. Marine sponges as Chloroflexi hot spots: genomic insights and high-resolution visualization of an abundant and diverse symbiotic clade. mSystems 3. https://doi.org/10.1128/msystems.00150-18.

Beck, H.E., Zimmermann, N.E., McVicar, T.R., Vergopolan, N., Berg, A., Wood, E.F., 2018. Present and future Köppen-Geiger climate classification maps at 1-km resolution. Sci Data 5, 180214. https://doi.org/10.1038/sdata.2018.214.

Bernhard, N., Moskwa, L.-M., Schmidt, K., Oeser, R.A., Aburto, F., Bader, M.Y., et al., 2018. Pedogenic and microbial interrelations to regional climate and local topography: new insights from a climate gradient (arid to humid) along the Coastal Cordillera of Chile. Catena 170, 335–355. https://doi.org/10.1016/j.catena.2018.06.018.

Bhat, S.V., Maughan, H., Cameron, A.D.S., Yost, C.K., 2022. Phylogenomic analysis of the genus Delftia reveals distinct major lineages with ecological specializations. Microb Genom 8, mgen000864. https://doi.org/10.1099/mgen.0.000864.

Bowman, R.A., Moir, J.O., 1993. Basic edta as an extractant for soil organic phosphorus. Soil Sci. Soc. Am. J. 57, 1516–1518. https://doi.org/10.2136/sssaj1993.03615995005700060020x.

Burt, R., 2004. Soil Survey Laboratory Methods Manual, Soil Survey Laboratory Investigations Report. National soil Survey Center, Natural Resources Conservation Service US Department of Agriculture Lincoln, Nebraska.

Callahan, B.J., McMurdie, P.J., Rosen, M.J., Han, A.W., Johnson, A.J.A., Holmes, S.P., 2016. DADA2: high-resolution sample inference from Illumina amplicon data. Nat. Methods 13, 581–583. https://doi.org/10.1038/nmeth.3869.

Carini, P., Marsden, P.J., Leff, J.W., Morgan, E.E., Strickland, M.S., Fierer, N., 2016. Relic DNA is abundant in soil and obscures estimates of soil microbial diversity. Nat. Microbiol. 2, 1–6. https://doi.org/10.1038/nmicrobiol.2016.242.

Carter, M.R., Gregorich, E.G. (Eds.), 2007. Soil Sampling and Methods of Analysis, 2nd edn. CRC Press, Boca Raton.

Ceccherini, M.T., Ascher, J., Agnelli, A., Borgogni, F., Pantani, O.L., Pietramellara, G., 2009. Experimental discrimination and molecular characterization of the extracellular soil DNA fraction. Antonie Van Leeuwenhoek 96, 653–657. https://doi.org/10.1007/s10482-009-9354-3.

Chase, A.B., Gomez-Lunar, Z., Lopez, A.E., Li, J., Allison, S.D., Martiny, A.C., et al., 2018. Emergence of soil bacterial ecotypes along a climate gradient. Environ. Microbiol. 20, 4112–4126. https://doi.org/10.1111/1462-2920.14405.

Csardi, G., Nepusz, T., et al., 2006. The igraph software package for complex network research. InterJournal, Complex Systems 1695, 1–9.

da Silva, A.C.R., Ferro, J.A., Reinach, F.C., Farah, C.S., Furlan, L.R., Quaggio, R.B., et al., 2002. Comparison of the genomes of two Xanthomonas pathogens with differing host specificities. Nature 417, 459–463. https://doi.org/10.1038/417459a.

Dedysh, S.N., Oren, A., 2019. Acidobacteriia. In: Bergey's Manual of Systematics of Archaea and Bacteria. John Wiley & Sons, Ltd, pp. 1–2. https://doi.org/10.1002/9781118960608.cbm00001.pub2.

Dusek, N., Hewitt, A.J., Schmidt, K.N., Bergholz, P.W., 2018. Landscape-scale factors affecting the prevalence of Escherichia coli in surface soil include land cover type, edge interactions, and soil pH. Appl. Environ. Microbiol. 84, e02714-17 https://doi.org/10.1128/AEM.02714-17.

Dyksma, S., Pester, M., 2023. Oxygen respiration and polysaccharide degradation by a sulfate-reducing acidobacterium. Nat. Commun. 14, 6337. https://doi.org/10.1038/s41467-023-42074-z.

Eisenlord, S.D., Zak, D.R., 2010. Simulated atmospheric nitrogen deposition alters actinobacterial community composition in forest soils. Soil Science Soc of Amer J 74, 1157–1166. https://doi.org/10.2136/sssaj2009.0240.

Ekelund, F., Rønn, R., Christensen, S., 2001. Distribution with depth of protozoa, bacteria and fungi in soil profiles from three Danish forest sites. Soil Biol. Biochem. 33, 475–481. https://doi.org/10.1016/S0038-0717(00)00188-7.

Erich, M.s., Plante, A.f., Fernández, J.m., Mallory, E.b., Ohno, T., 2012. Effects of profile depth and management on the composition of labile and total soil organic matter. Soil Sci. Soc. Am. J. 76, 408–419. https://doi.org/10.2136/sssaj2011.0273.

Fang, J., Jin, L., Meng, Q., Wang, D., Lin, D., 2021. Interactions of extracellular DNA with aromatized biochar and protection against degradation by DNase I. J. Environ. Sci. 101, 205–216. https://doi.org/10.1016/j.jes.2020.08.017.

Garrido-Benavent, I., Pérez-Ortega, S., Durán, J., Ascaso, C., Pointing, S.B., Rodríguez-Cielos, R., et al., 2020. Differential colonization and succession of microbial communities in rock and soil substrates on a maritime Antarctic glacier forefield. Front. Microbiol. 11 https://doi.org/10.3389/fmicb.2020.00126.

Genderjahn, S., Alawi, M., Mangelsdorf, K., Horn, F., Wagner, D., 2018. Desiccation- and saline-tolerant bacteria and archaea in Kalahari Pan sediments. Front. Microbiol. 9 https://doi.org/10.3389/fmicb.2018.02082.

Genderjahn, S., Lewin, S., Horn, F., Schleicher, A.M., Mangelsdorf, K., Wagner, D., 2021. Living lithic and sublithic bacterial communities in Namibian drylands. Microorganisms 9, 235. https://doi.org/10.3390/microorganisms9020235.

Geological Map of South America at a Scale of 1:5M, 2019. Servicio Geológico Colombiano. https://doi.org/10.32685/10.143.2019.929.

Gonçalves de Chaves, M., Silva, G.G.Z., Rossetto, R., Edwards, R.A., Tsai, S.M., Navarrete, A.A., 2019. Acidobacteria subgroups and their metabolic potential for carbon degradation in sugarcane soil amended with vinasse and nitrogen fertilizers. Front. Microbiol. 10 https://doi.org/10.3389/fmicb.2019.01680.

Goodfellow, M., Williams, S.T., 1983. Ecology of Actinomycetes. Ann. Rev. Microbiol. 37, 189–216. https://doi.org/10.1146/annurev.mi.37.100183.001201.

Gorelick, N., Hancher, M., Dixon, M., Ilyushchenko, S., Thau, D., Moore, R., 2017. Google Earth Engine: planetary-scale geospatial analysis for everyone. Remote Sens. Environ. https://doi.org/10.1016/j.rse.2017.06.031.

Guerra, C.A., Bardgett, R.D., Caon, L., Crowther, T.W., Delgado-Baquerizo, M., Montanarella, L., et al., 2021. Tracking, targeting, and conserving soil biodiversity. Science 371, 239–241. https://doi.org/10.1126/science.abd7926.

Haile, J., Holdaway, R., Oliver, K., Bunce, M., Gilbert, M.T.P., Nielsen, R., et al., 2007. Ancient DNA chronology within sediment deposits: are paleobiological reconstructions possible and is DNA leaching a factor? Mol. Biol. Evol. 24, 982–989. https://doi.org/10.1093/molbev/msm016.

Hao, J., Chai, Y.N., Lopes, L.D., Ordóñez, R.A., Wright, E.E., Archontoulis, S., et al., 2021. The effects of soil depth on the structure of microbial communities in agricultural soils in Iowa (United States). Appl. Environ. Microbiol. 87, e02673-20 https://doi.org/10.1128/AEM.02673-20.

Harrell Jr., F.E., 2021. Hmisc: Harrell miscellaneous. Available at: https://CRAN.R-project.org/package=Hmisc.

Hill, P., Krištůfek, V., Dijkhuizen, L., Boddy, C., Kroetsch, D., van Elsas, J.D., 2011. Land use intensity controls Actinobacterial community structure. Microb. Ecol. 61, 286–302. https://doi.org/10.1007/s00248-010-9752-0.

Hoeksma, P., Aarnink, A.J.A., Ogink, N., 2015. Effect of Temperature and Relative Humidity on the Survival of Airborne bacteria = Effect van temperatuur en relatieve luchtvochtig-heid op de overleving van bacteriën in de lucht. Wageningen UR Livestock Research.

Holmalahti, J., von Wright, A., Raatikainen, O., 1994. Variations in the spectra of biological activities of actinomycetes isolated from different soils. Lett. Appl. Microbiol. 18, 144–146. https://doi.org/10.1111/j.1472-765X.1994.tb00829.x.

Holmes, A.J., Bowyer, J., Holley, M.P., O'Donoghue, M., Montgomery, M., Gillings, M.R., 2000. Diverse, yet-to-be-cultured members of the Rubrobacter subdivision of the Actinobacteria are widespread in Australian arid soils. FEMS Microbiol. Ecol. 33, 111–120. https://doi.org/10.1111/j.1574-6941.2000.tb00733.x.

Horstmann, L., Lipus, D., Bartholomäus, A., Arens, F., Airo, A., Ganzert, L., et al., 2024. Persistent microbial communities in hyperarid subsurface habitats of the Atacama Desert: insights from intracellular DNA analysis. PNAS Nexus 3, 123. https://doi.org/10.1093/pnasnexus/pgae123.

Huang, J., Sheng, X.-F., Xi, J., He, L.-Y., Huang, Z., Wang, Q., et al., 2014. Depth-related changes in community structure of culturable mineral weathering bacteria and in weathering patterns caused by them along two contrasting soil profiles. Appl. Environ. Microbiol. 80, 29–42. https://doi.org/10.1128/AEM.02335-13.

Ibáñez de Aldecoa, A.L., Zafra, O., González-Pastor, J.E., 2017. Mechanisms and regulation of extracellular DNA release and its biological roles in microbial communities. Front. Microbiol. 8, 1390. https://doi.org/10.3389/fmicb.2017.01390.

Jones, R.T., 2015. A comprehensive survey of soil rhizobiales diversity using high-throughput DNA sequencing. Biological Nitrogen Fixation 769–776. https://doi.org/10.1002/9781119053095.ch76.

Karimi, E., Slaby, B.M., Soares, A.R., Blom, J., Hentschel, U., Costa, R., 2018. Metagenomic binning reveals versatile nutrient cycling and distinct adaptive features in alphaproteobacterial symbionts of marine sponges. FEMS Microbiol. Ecol. 94, fiy074 https://doi.org/10.1093/femsec/fiy074.

Kim, H.-S., Lee, S.-H., Jo, H.Y., Finneran, K.T., Kwon, M.J., 2021. Diversity and composition of soil Acidobacteria and Proteobacteria communities as a bacterial indicator of past land-use change from forest to farmland. Sci. Total Environ. 797, 148944 https://doi.org/10.1016/j.scitotenv.2021.148944.

Kolde, R., 2019. pheatmap: pretty heatmaps. Available at: https://CRAN.R-project.org/package=pheatmap.

Kulichevskaya, I.S., Naumoff, D.G., Ivanova, A.A., Rakitin, A.L., Dedysh, S.N., 2019. Detection of chitinolytic capabilities in the freshwater Planctomycete Planctomicrobium piriforme. Microbiology 88, 423–432. https://doi.org/10.1134/S0026261719040076.

Ladau, J., Shi, Y., Jing, X., He, J.-S., Chen, L., Lin, X., et al., 2018. Existing climate change will lead to pronounced shifts in the diversity of soil prokaryotes. mSystems 3. https://doi.org/10.1128/msystems.00167-18.

Langfelder, P., Horvath, S., 2008. WGCNA: an R package for weighted correlation network analysis. BMC Bioinformatics 9, 559. https://doi.org/10.1186/1471-2105-9-559.

Langwig, M.V., De Anda, V., Dombrowski, N., Seitz, K.W., Rambo, I.M., Greening, C., et al., 2022. Large-scale protein level comparison of Deltaproteobacteria reveals cohesive metabolic groups. ISME J. 16, 307–320. https://doi.org/10.1038/s41396-021-01057-y.

Lavahun, M.F.E., Joergensen, R.G., Meyer, B., 1996. Activity and biomass of soil microorganisms at different depths. Biol. Fertil. Soils 23, 38–42. https://doi.org/10.1007/BF00335816.

Lee, K.C., Caruso, T., Archer, S.D.J., Gillman, L.N., Lau, M.C.Y., Cary, S.C., et al., 2018. Stochastic and deterministic effects of a moisture gradient on soil microbial communities in the McMurdo Dry Valleys of Antarctica. Front. Microbiol. 9 https://doi.org/10.3389/fmicb.2018.02619.

Levy-Booth, D.J., Campbell, R.G., Gulden, R.H., Hart, M.M., Powell, J.R., Klironomos, J. N., et al., 2007. Cycling of extracellular DNA in the soil environment. Soil Biol. Biochem. 39, 2977–2991. https://doi.org/10.1016/j.soilbio.2007.06.020.

Li, Q., Zhang, D., Cheng, H., Song, Z., Ren, L., Hao, B., et al., 2021a. Chloropicrin alternated with dazomet improved the soil's physicochemical properties, changed microbial communities and increased strawberry yield. Ecotoxicol. Environ. Saf. 220, 112362 https://doi.org/10.1016/j.ecoenv.2021.112362.

Li, Y., Shahbaz, M., Zhu, Z., Deng, Y., Tong, Y., Chen, L., et al., 2021b. Oxygen availability determines key regulators in soil organic carbon mineralisation in paddy soils. Soil Biol. Biochem. 153, 108106 https://doi.org/10.1016/j.soilbio.2020.108106.

Magoč, T., Salzberg, S.L., 2011. FLASH: fast length adjustment of short reads to improve genome assemblies. Bioinformatics 27, 2957–2963. https://doi.org/10.1093/bioinformatics/btr507.

Medina Caro, D., Horstmann, L., Ganzert, L., Oses, R., Friedl, T., Wagner, D., 2023. An improved method for intracellular DNA (iDNA) recovery from terrestrial environments. MicrobiologyOpen 12, e1369. https://doi.org/10.1002/mbo3.1369.

Meier, L.A., Krauze, P., Prater, I., Horn, F., Schaefer, C.E.G.R., Scholten, T., et al., 2019. Pedogenic and microbial interrelation in initial soils under semiarid climate on James Ross Island, Antarctic Peninsula region. Biogeosciences 16, 2481–2499. https://doi.org/10.5194/bg-16-2481-2019.

Mesa, V., Gallego, J.L.R., González-Gil, R., Lauga, B., Sánchez, J., Méndez-García, C., et al., 2017. Bacterial, archaeal, and eukaryotic diversity across distinct microhabitats in an acid mine drainage. Front. Microbiol. 8 https://doi.org/10.3389/fmicb.2017.01756.

Miranda, K.M., Espey, M.G., Wink, D.A., 2001. A rapid, simple spectrophotometric method for simultaneous detection of nitrate and nitrite. Nitric Oxide 5, 62–71. https://doi.org/10.1006/niox.2000.0319.

Morrissey, E.M., McHugh, T.A., Preteska, L., Hayer, M., Dijkstra, P., Hungate, B.A., et al., 2015. Dynamics of extracellular DNA decomposition and bacterial community composition in soil. Soil Biol. Biochem. 86, 42–49. https://doi.org/10.1016/j.soilbio.2015.03.020.

Mundra, S., Kjønaas, O.J., Morgado, L.N., Krabberød, A.K., Ransedokken, Y., Kauserud, H., 2021. Soil depth matters: shift in composition and inter-kingdom co-occurrence patterns of microorganisms in forest soils. FEMS Microbiol. Ecol. 97, fiab022 https://doi.org/10.1093/femsec/fiab022.

Naylor, D., Sadler, N., Bhattacharjee, A., Graham, E.B., Anderton, C.R., McClure, R., et al., 2020. Soil microbiomes under climate change and implications for carbon cycling. Annu. Rev. Environ. Resour. 45, 29–59. https://doi.org/10.1146/annurev-environ-012320-082720.

Nercessian, O., Noyes, E., Kalyuzhnaya, M.G., Lidstrom, M.E., Chistoserdova, L., 2005. Bacterial populations active in metabolism of C1 compounds in the sediment of Lake Washington, a freshwater lake. Appl. Environ. Microbiol. 71, 6885–6899. https://doi.org/10.1128/AEM.71.11.6885-6899.2005.

O'Brien, F.J.M., Almaraz, M., Foster, M.A., Hill, A.F., Huber, D.P., King, E.K., et al., 2019. Soil salinity and pH drive soil bacterial community composition and diversity along a lateritic slope in the Avon River Critical Zone Observatory. Western Australia. Frontiers in Microbiology 10. https://doi.org/10.3389/fmicb.2019.01486.

Oeser, R.A., Stroncik, N., Moskwa, L.-M., Bernhard, N., Schaller, M., Canessa, R., et al., 2018. Chemistry and microbiology of the Critical Zone along a steep climate and vegetation gradient in the Chilean Coastal Cordillera. CATENA 170, 183–203. https://doi.org/10.1016/j.catena.2018.06.002.

Ogram, A., Sayler, G.S., Barkay, T., 1987. The extraction and purification of microbial DNA from sediments. J. Microbiol. Methods 7, 57–66. https://doi.org/10.1016/0167-7012(87)90025-X.

Oksanen, J., Simpson, G.L., Blanchet, F.G., Kindt, R., Legendre, P., Minchin, P.R., et al., 2022. vegan: community ecology package. Available at: https://CRAN.R-project.org/package=vegan.

Oren, A., 2014. The family Xanthobacteraceae. In: The Prokaryotes, pp. 709–726. https://doi.org/10.1007/978-3-642-30197-1_258.

Pathan, S.I., Arfaioli, P., Ceccherini, M.T., Ascher-Jenull, J., Nannipieri, P., Pietramellara, G., et al., 2021a. Physical protection of extracellular and intracellular DNA in soil aggregates against simulated natural oxidative processes. Appl. Soil Ecol. 165, 104002 https://doi.org/10.1016/j.apsoil.2021.104002.

Pathan, S.I., Arfaioli, P., Taskin, E., Ceccherini, M.T., Puglisi, E., Pietramellara, G., 2021b. The extracellular DNA can baffle the assessment of soil bacterial community, but the effect varies with microscale spatial distribution. FEMS Microbiol. Lett. 368, fnab074 https://doi.org/10.1093/femsle/fnab074.

Patzner, M.S., Mueller, C.W., Malusova, M., Baur, M., Nikeleit, V., Scholten, T., et al., 2020. Iron mineral dissolution releases iron and associated organic carbon during permafrost thaw. Nat. Commun. 11, 6329. https://doi.org/10.1038/s41467-020-20102-6.

Paul, E., 2014. Soil Microbiology, Ecology and Biochemistry. Academic Press.

Pedersen, T.L., 2020. patchwork: the composer of plots. Available at: https://CRAN.R-project.org/package=patchwork.

Pedersen, T.L., 2022. ggraph: an implementation of grammar of graphics for graphs and networks. Available at: https://CRAN.R-project.org/package=ggraph.

Pedersen, M.W., De Sanctis, B., Saremi, N.F., Sikora, M., Puckett, E.E., Gu, Z., et al., 2021. Environmental genomics of Late Pleistocene black bears and giant short-faced bears. Curr. Biol. 31, 2728–2736.e8. https://doi.org/10.1016/j.cub.2021.04.027.

Puche, E., Rojo, C., Segura, M., Rodrigo, M.A., 2021. Macrophyte meadows mediate the response of the sediment microbial community to ultraviolet radiation. Hydrobiologia 848, 4569–4583. https://doi.org/10.1007/s10750-021-04662-2.

Quast, C., Pruesse, E., Yilmaz, P., Gerken, J., Schweer, T., Yarza, P., et al., 2013. The SILVA ribosomal RNA gene database project: improved data processing and web-based tools. Nucleic Acids Res. 41, D590–D596. https://doi.org/10.1093/nar/gks1219.

R Core Team, 2022. R: A Language and Environment for Statistical Computing. R Foundation for Statistical Computing. Available at: https://www.R-project.org/.

Rahimlou, S., Bahram, M., Tedersoo, L., 2021. Phylogenomics reveals the evolution of root nodulating alpha- and beta-Proteobacteria (rhizobia). Microbiol. Res. 250, 126788 https://doi.org/10.1016/j.micres.2021.126788.

Reis, F., Soares-Castro, P., Costa, D., Tavares, R.M., Baptista, P., Santos, P.M., et al., 2019. Climatic impacts on the bacterial community profiles of cork oak soils. Appl. Soil Ecol. 143, 89–97. https://doi.org/10.1016/j.apsoil.2019.05.031.

Roberts, D.W., 2023. labdsv: ordination and multivariate analysis for ecology. Available at: https://CRAN.R-project.org/package=labdsv.

Rodriguez, V., Moskwa, L.-M., Oses, R., Kühn, P., Riveras-Muñoz, N., Seguel, O., et al., 2022. Impact of climate and slope aspects on the composition of soil bacterial communities involved in pedogenetic processes along the Chilean Coastal Cordillera. Microorganisms 10, 847. https://doi.org/10.3390/microorganisms10050847.

Rodríguez, V., Bartholomäus, A., Witzgall, K., Riveras-Muñoz, N., Oses, R., Liebner, S., et al., 2024. Microbial impact on initial soil formation in arid and semiarid environments under simulated climate change. Front. Microbiol. 15 https://doi.org/10.3389/fmicb.2024.1319997.

Rofner, C., Peter, H., Catalán, N., Drewes, F., Sommaruga, R., Pérez, M.T., 2017. Climate-related changes of soil characteristics affect bacterial community composition and function of high altitude and latitude lakes. Glob. Chang. Biol. 23, 2331–2344. https://doi.org/10.1111/gcb.13545.

RStudio Team, 2021. RStudio: Integrated Development Environment for R. Available at: http://www.rstudio.com/.

Ruan, Y., Kuzyakov, Y., Liu, X., Zhang, X., Xu, Q., Guo, J., et al., 2023. Elevated temperature and CO2 strongly affect the growth strategies of soil bacteria. Nat. Commun. 14, 391. https://doi.org/10.1038/s41467-023-36086-y.

Saary, P., Forslund, K., Bork, P., Hildebrand, F., 2017. RTK: efficient rarefaction analysis of large datasets. Bioinformatics 33, 2594–2595. https://doi.org/10.1093/bioinformatics/btx206.

Sánchez-Marañón, M., Miralles, I., Aguirre-Garrido, J.F., Anguita-Maeso, M., Millán, V., Ortega, R., et al., 2017. Changes in the soil bacterial community along a pedogenic gradient. Sci. Rep. 7, 14593 https://doi.org/10.1038/s41598-017-15133-x.

Schellenberger, S., Kolb, S., Drake, H.L., 2010. Metabolic responses of novel cellulolytic and saccharolytic agricultural soil Bacteria to oxygen. Environ. Microbiol. 12, 845–861. https://doi.org/10.1111/j.1462-2920.2009.02128.x.

Schulze-Makuch, D., Wagner, D., Kounaves, S. P., Mangelsdorf, K., Devine, K. G., Vera, J.-P. de, et al. (2018). Transitory microbial habitat in the hyperarid Atacama Desert. PNAS 115, 2670–2675. doi:https://doi.org/10.1073/pnas.1714341115.

Schulze-Makuch, D., Lipus, D., Arens, F.L., Baqué, M., Bornemann, T.L.V., de Vera, J.-P., et al., 2021. Microbial hotspots in lithic microhabitats inferred from DNA fractionation and metagenomics in the Atacama Desert. Microorganisms 9, 1038. https://doi.org/10.3390/microorganisms9051038.

Shang, C., Zelazny, L.W., 2008. Selective dissolution techniques for mineral analysis of soils and sediments. In: Methods of Soil Analysis Part 5—Mineralogical Methods. John Wiley & Sons, Ltd, pp. 33–80. https://doi.org/10.2136/sssabookser5.5.c3.
Sharma, P., Kalita, M.C., Thakur, D., 2016. Broad spectrum antimicrobial activity of Forest-derived soil Actinomycete, Nocardia sp. PB-52. Front. Microbiol. 7 https://doi.org/10.3389/fmicb.2016.00347.
Sharrar, A.M., Crits-Christoph, A., Méheust, R., Diamond, S., Starr, E.P., Banfield, J.F., 2020. Bacterial secondary metabolite biosynthetic potential in soil varies with phylum, depth, and vegetation type. mBio 11, e00416-20. https://doi.org/10.1128/mBio.00416-20.
Six, J., Bossuyt, H., Degryze, S., Denef, K., 2004. A history of research on the link between (micro)aggregates, soil biota, and soil organic matter dynamics. Soil Tillage Res. 79, 7–31. https://doi.org/10.1016/j.still.2004.03.008.
Smith, P., Cotrufo, M.F., Rumpel, C., Paustian, K., Kuikman, P.J., Elliott, J.A., et al., 2015. Biogeochemical cycles and biodiversity as key drivers of ecosystem services provided by soils. Soil 1, 665–685. https://doi.org/10.5194/soil-1-665-2015.
Spain, A.M., Krumholz, L.R., Elshahed, M.S., 2009. Abundance, composition, diversity and novelty of soil Proteobacteria. ISME J. 3, 992–1000. https://doi.org/10.1038/ismej.2009.43.
Stone, B.W., Li, J., Koch, B.J., Blazewicz, S.J., Dijkstra, P., Hayer, M., et al., 2021. Nutrients cause consolidation of soil carbon flux to small proportion of bacterial community. Nat. Commun. 12, 3381. https://doi.org/10.1038/s41467-021-23676-x.
Suzuki, K., 2015. Rubrobacter. In: Bergey's Manual of Systematics of Archaea and Bacteria. John Wiley & Sons, Ltd, pp. 1–6. https://doi.org/10.1002/9781118960608.gbm00224.
Székely, A.J., Langenheder, S., 2014. The importance of species sorting differs between habitat generalists and specialists in bacterial communities. FEMS Microbiol. Ecol. 87, 102–112. https://doi.org/10.1111/1574-6941.12195.
Szoboszlay, M., Tebbe, C.C., 2021. Hidden heterogeneity and co-occurrence networks of soil prokaryotic communities revealed at the scale of individual soil aggregates. MicrobiologyOpen 10, e1144. https://doi.org/10.1002/mbo3.1144.
Tao, X., Feng, J., Yang, Y., Wang, G., Tian, R., Fan, F., et al., 2020. Winter warming in Alaska accelerates lignin decomposition contributed by Proteobacteria. Microbiome 8, 84. https://doi.org/10.1186/s40168-020-00838-5.
Thomas, G.W., 1996. Soil pH and soil acidity. Methods of Soil Analysis: Part 3 Chemical Methods 5, 475–490.
Thomsen, P.F., Willerslev, E., 2015. Environmental DNA – an emerging tool in conservation for monitoring past and present biodiversity. Biol. Conserv. 183, 4–18. https://doi.org/10.1016/j.biocon.2014.11.019.
Tibbett, M., Gil-Martínez, M., Fraser, T., Green, I.D., Duddigan, S., De Oliveira, V.H., et al., 2019. Long-term acidification of pH neutral grasslands affects soil biodiversity, fertility and function in a heathland restoration. Catena 180, 401–415. https://doi.org/10.1016/j.catena.2019.03.013.
Torti, A., Lever, M.A., Jørgensen, B.B., 2015. Origin, dynamics, and implications of extracellular DNA pools in marine sediments. Mar. Genomics 24, 185–196. https://doi.org/10.1016/j.margen.2015.08.007.
van Gestel, N.C., Reischke, S., Bååth, E., 2013. Temperature sensitivity of bacterial growth in a hot desert soil with large temperature fluctuations. Soil Biol. Biochem. 65, 180–185. https://doi.org/10.1016/j.soilbio.2013.05.016.
Van Horn, D.J., Okie, J.G., Buelow, H.N., Gooseff, M.N., Barrett, J.E., Takacs-Vesbach, C. D., 2014. Soil microbial responses to increased moisture and organic resources along a salinity gradient in a polar desert. Appl. Environ. Microbiol. 80, 3034–3043. https://doi.org/10.1128/AEM.03414-13.
Ventosa, A., de la Haba, R.R., Arahal, D.R., Sánchez-Porro, C., 2021. Halomonas. In: Bergey's Manual of Systematics of Archaea and Bacteria. John Wiley & Sons, Ltd, pp. 1–111. https://doi.org/10.1002/9781118960608.gbm01190.pub2.
Watanabe, F.S., Olsen, S.R., 1965. Test of an ascorbic acid method for determining phosphorus in water and NaHCO3 extracts from soil. Soil Sci. Soc. Am. J. 29, 677–678. https://doi.org/10.2136/sssaj1965.03615995002900060025x.
Wei, T., Simko, V., 2021. R package "corrplot": visualization of a correlation matrix. Available at: https://github.com/taiyun/corrplot.
Wickham, H., 2016. ggplot2: Elegant Graphics for Data Analysis. Springer-Verlag, New York. Available at: https://ggplot2.tidyverse.org.
Wickham, H., Averick, M., Bryan, J., Chang, W., McGowan, L., François, R., et al., 2019. Welcome to the Tidyverse. JOSS 4, 1686. https://doi.org/10.21105/joss.01686.
Wilhelm, R.C., Singh, R., Eltis, L.D., Mohn, W.W., 2019. Bacterial contributions to delignification and lignocellulose degradation in forest soils with metagenomic and quantitative stable isotope probing. ISME J. 13, 413–429. https://doi.org/10.1038/s41396-018-0279-6.
Xu, T., Chen, X., Hou, Y., Zhu, B., 2021. Changes in microbial biomass, community composition and diversity, and functioning with soil depth in two alpine ecosystems on the Tibetan plateau. Plant Soil 459, 137–153. https://doi.org/10.1007/s11104-020-04712-z.
Yan, Y., Klinkhamer, P.G.L., van Veen, J.A., Kuramae, E.E., 2019. Environmental filtering: a case of bacterial community assembly in soil. Soil Biol. Biochem. 136, 107531 https://doi.org/10.1016/j.soilbio.2019.107531.
Yang, X.-D., Ali, A., Xu, Y.-L., Jiang, L.-M., Lv, G.-H., 2019. Soil moisture and salinity as main drivers of soil respiration across natural xeromorphic vegetation and agricultural lands in an arid desert region. Catena 177, 126–133. https://doi.org/10.1016/j.catena.2019.02.015.
Yu, H., Li, L., Ma, Q., Liu, X., Li, Y., Wang, Y., et al., 2023. Soil microbial responses to large changes in precipitation with nitrogen deposition in an arid ecosystem. Ecology 104, e4020. https://doi.org/10.1002/ecy.4020.
Zhang, K., Shi, Y., Lu, H., He, M., Huang, W., Siemann, E., 2022. Soil bacterial communities and co-occurrence changes associated with multi-nutrient cycling under rice-wheat rotation reclamation in coastal wetland. Ecol. Indic. 144, 109485 https://doi.org/10.1016/j.ecolind.2022.109485.
Zhou, J., Deng, Y., Shen, L., Wen, C., Yan, Q., Ning, D., et al., 2016. Temperature mediates continental-scale diversity of microbes in forest soils. Nat. Commun. 7, 12083 https://doi.org/10.1038/ncomms12083.